Karimzadeh et al., ***BioImpacts.*** 2026;16:33736
doi:10.34172/bi.33736
https://bi.tbzmed.ac.ir/

Advancements in the detection of emerging chemical contaminants using paper microfluidics enhanced by nanomaterials and artificial intelligence

Saeid Karimzadeh[1,2#], Mansour Mahmoudpour[3#], Mir-Michael Mousavi[4], Zahra Karimzadeh[1*]

[1]Research Center for Pharmaceutical Nanotechnology, Biomedicine Institute, Tabriz University of Medical Sciences, Tabriz, Iran
[2]Faculty of Mechanical Engineering, University of Tabriz, Tabriz, Iran
[3]Miandoab Faculty of Medical Sciences, Urmia University of Medical Sciences, Urmia, Iran
[4]Food Safety Research Center (Salt), Semnan University of Medical Sciences, Semnan, Iran

Article Info

Article Type:
Review

Article History:
Received: 9 Apr. 2026
Revised: 27 May 2026
Accepted: 28 May 2026
ePublished: 15 Sep. 2026

Keywords:
Nanomaterials
Microfluidics
Chemical contaminants
Food safety
Environmental samples
Point-of-care test

Abstract

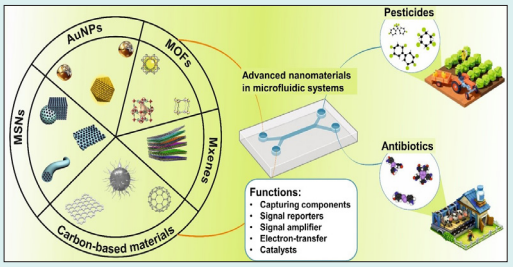

Recent advancements in nanomaterials (NMs) and microfluidic technologies are crucial for improving the detection of chemical contaminants in food and environmental samples. Integrating NMs into microfluidic systems significantly enhances the sensitivity and selectivity of these detection methods, effectively meeting the urgent need for efficient monitoring of harmful pollutants resulting from unsustainable growth practices. This review focuses on the development of NM-based microfluidic systems specifically designed for the rapid detection of chemical pollutants. It emphasizes the use of various nanomaterials with zero-, one-, two-, and three-dimensional structures (0D, 1D, 2D, and 3D). In addition to summarizing recent research, this review presents a comparative analysis of various sensing mechanisms, namely fluorescence, colorimetric, SERS, electrochemical, and chemiluminescence, evaluating them in terms of stability, sensitivity, scalability, reproducibility, and real-world applicability. Moreover, the integration of NM-based microfluidic systems with modern technologies like artificial intelligence (AI) and the Internet of Medical Things (IoMT) has led to the progress of 5th generation smart biosensors featuring lab-on-a-chip, point-of-care, and wearable capabilities. This review highlights the critical role of these advanced systems in safeguarding food safety and environmental health by describing their unique characteristics and functionalities. Additionally, it discusses the challenges and future research directions in this important field.

Introduction

In recent decades, urbanization, the extensive use of chemicals in agricultural practices, and adverse environmental factors have collectively contributed to a rising incidence of food-related health issues worldwide. This situation underscores the significant emphasis and collaborative efforts by key stakeholders in the food industry, including food companies and agro-allied organizations, to actively monitor and ensure food safety.[1] It is essential to develop rapid and efficient methods for assessing food safety to ensure the quality and wholesomeness of food products. The use of chemicals in the food industry serves multiple purposes, some of which are critical for preservation and improving production processes. Furthermore, the application of certain chemicals in agricultural practices has made food products susceptible to significant health risks, as evidenced by their accumulation in the food supply.

Conventional methods, such as gas chromatography (GC), combined with gas chromatography mass spectrometry (GC-MS), high-performance liquid chromatography (HPLC), nuclear magnetic resonance (NMR) spectroscopy, and enzyme-linked immunosorbent assay (ELISA), are influential and extensively utilized to carry out food safety and quality assessments.[2] These methods render great accuracy. Nevertheless, they

*Corresponding author: Zahra Karimzadeh, Email: karimzadeh94z@gmail.com
#These authors contributed equally to this work and should be regarded as co-first authors.

Review Highlights

- Nanomaterial-integrated microfluidic systems for rapid, sensitive, and selective detection of chemical contaminants in food and environmental samples.
- Comprehensive review of 0D–3D nanomaterial-based microfluidic systems and integration of AI and IoMT into smart lab-on-chip and wearable biosensors.

need expensive instrumentation, trained workers, and complicated measurements, time-consuming.[3] Besides, they are not sufficient to determine numerous chemical pollutants in today's foodstuffs, frequently in low quantities. Thereinto, rapid, cost-effective, and practical sensing with a high-efficiency technique that could be exploited at an industrial scale is in demand.

Newly established diagnostic approaches can be easily integrated with handheld, portable tools, enabling on-site sample analysis.[4] In today's world, microfluidics has ignited a surge of unprecedented attention as a versatile and powerful technology.[5-7] Beside environmental monitoring and food safety, microfluidic systems have exhibited remarkable applicability in pharmaceutical and medical applications. Due to their high sensitivity, rapid analysis, low sample consumption, and portability, microfluidic platforms have been widely explored for personalized medicine, drug screening, disease diagnostics, and therapeutic monitoring. The potential of a microfluidic 'lab-on-a-chip' system is being fulfilled, drawing on properties like no need for expensive diagnostic devices, low reagent, and sample consumption, short process times owing to little diffusion distances, and the capability to perform numerous stages of the diagnostic workflow on the small footprint tool (sample-in-answer-out) for the food safety and health care fields.[8]

The functionality of microfluidic systems is influenced by a range of critical design parameters that govern fluid transport characteristics and analytical performance.[9,10] Key among these is channel geometry—including dimensions such as width, height, and overall architecture—which affects flow resistance, residence time, and mixing efficiency. In paper-based devices, substrate properties such as pore size, thickness, and fiber morphology control capillary-driven fluid flow.[11] Additionally, fluidic parameters like applied pressure, flow rate, and surface tension modulate transport dynamics. Surface wettability and intrinsic material properties (e.g., glass, polydimethylsiloxane, cellulose, and various polymers) further impact analyte adsorption, nonspecific binding, and chemical compatibility. Reaction-specific factors, including reaction kinetics, mixing efficiency, and diffusion rates, along with environmental variables such as temperature, pH, and sample viscosity, are also critical determinants of detecting reproducibility and accuracy. Therefore, the systematic optimization of these interrelated parameters is essential to develop analytical systems that are sensitive, robust, and reliable.

The incorporation of nanomaterials (NMs) into microfluidic systems has further enhanced analytical performance, enabling the development of highly efficient lab-on-chip platforms. The nano size of NPs enables them to flow in the micro-channels liberally and easily incorporate into the microfluidic platforms.[12] Besides, NMs possess numerous gorgeous features, *e.g.*, magnetic, catalytic, electrochemical, or optical properties, easy functionalization, and a high surface area-to-volume ratio. They can function as signal amplifiers, signal reporters, capturing elements, catalysts, or electron-transfer mediators, thereby simplifying analytical reactions, enhancing target molecule detection, and promoting signal transmission. This significantly improves the performance of microfluidic devices, particularly in terms of selectivity and sensitivity. In summary, integrating NMs with flexible surface functionalization and specific morphologies into microfluidic systems offers promising opportunities for the sensitive and rapid detection of chemical contaminants. As microfluidic technology utilizing NMs has significantly advanced, several review studies have been published in recent years to elucidate its progress and evaluate its potential applications.[13-16] Despite significant advancements in NM-based microfluidics for the detection of chemical contaminants, most previous studies have focused on individual analytical platforms conventional sensing mechanisms, or specific NMs and a comprehensive overview of these developments has not yet been presented.

In this study, we present a comprehensive overview of recent advancements in microfluidic substrates that employ various NMs for detecting chemical contaminants in modern food products. This study seeks to delineate the properties of various NMs and their methods of incorporation into microfluidic technology. The unique feature of this review is the systematic classification of NMs based on their dimensional architectures (0D, 1D, 2D, and 3D) and the assessment of their functional roles in improving sensing performance within microfluidic platforms in the detection of pesticide residues, antibiotic residues, and heavy metals (Scheme 1). Furthermore, it highlights current advances in smart NM-based microfluidic biosensors integrated with point-of-care systems, lab-on-chip technologies, wearable devices, AI, and IoMT. By connecting microfluidic design, material engineering, and digital healthcare technologies, it provides future perspectives for the advancement of next-generation intelligent sensing systems for environmental monitoring and food safety.

Nanomaterials integrated into microfluidic (bio)sensing

NMs with varying dimensions typically demonstrate distinct benefits and drawbacks. NMs with 0D features, characterized by their extremely small sizes, offer the benefits of simple manipulation, easy synthesis, and distinctive electronic, optical, or magnetic properties. They have the capability to be attached to chemical contaminants, and the resulting functionalized NPs

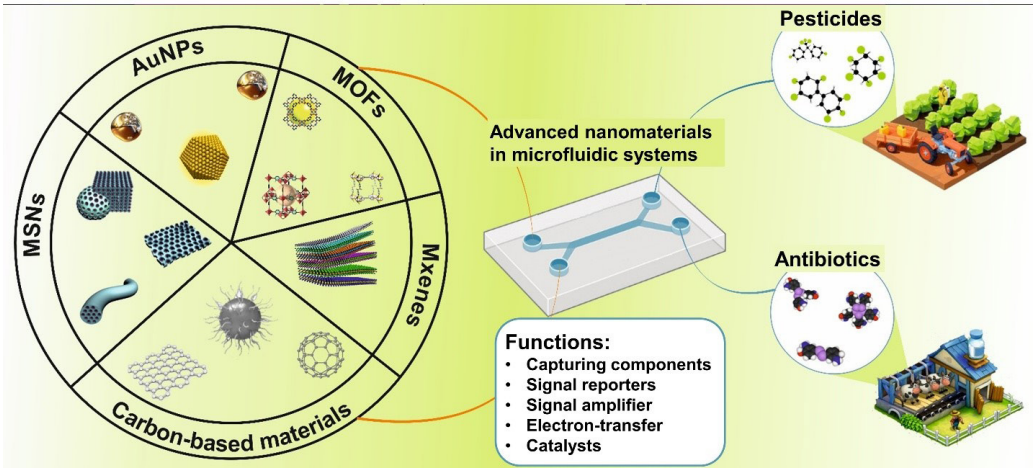

Scheme 1. Schematic representation for paper microfluidic sensors enhanced by nanomaterials in determination of chemical contaminants.

can be utilized as food safety markers.[17] However, they frequently suffer from easy aggregation and poor stability.[18] One-dimensional NMs possess a microscale length and nanosized diameter, donating them with mechanical strength and high surface-to-volume ratio, which is favorable for the fabrication of larger nanostructured materials.[19] However, the growth of 1D NMs is intricate and typically requires precise synthetic methods, which ultimately dictate their uniformity.[20] Two-dimensional NMs such as graphene exhibit attractive chemical and physical characteristics, comprising excellent thermal/electrical conductivity, high specific surface area, stability, flexibility, and easy biological/chemical functionalization.[21,22] But they are easy to restack, costly to produce, and vulnerable to the oxidative atmosphere.[23] 3D NMs might comprise collection nanotubes, nanowires, or varied distributions of NPs, enabling the integration of diverse NM properties to achieve more complex functionalities. A diverse range of 3D NMs exists, with varying sizes and shapes, offering diverse potential applications in detection.[24] Nevertheless, their synthesis procedures are relatively complex, lack standardization, and are expensive.[25]

The integration of NMs into chips is primarily determined by their specific functions in the analysis process. In brief, NMs are typically incorporated as signal probes directly onto chips through injection with a pump, drop casting, or modification on the electrodes for electrical detection.[26] Whereas capture probes made of NMs are usually modified within the channels of microfluidic chips through in-situ synthesis, self-assembly, etc., except for magnetic materials that can be manipulated using an external magnetic field.[27] In this regard, we will explore the common NMs used in microfluidic systems for analyzing chemical contaminants in food, as well as their functions and integration techniques in microfluidic systems, which is summarized in Table 1.

Zero-dimensional NMs

Zero-dimensional NMs are generally NPs with sizes less than 100 nm. To date, many 0D NMs, such as metal NPs, quantum dots (QDs), and magnetic NPs (MNPs), have been thoroughly investigated and utilized in microfluidic biosensors.[63] Their distinctive magnetic, optical, or electrical qualities render them significant assets in the development of microfluidics for the analysis of food and environmental samples.[64]

Metal NPs

Metal NPs typically serve as signal-transduction and/or target-capturing factors in microfluidic platforms.[65] The NMs are incorporated into the microfluidic systems through self-assembly, in-situ synthesis, or directly loading suspension into microfluidic chips after or before mixing with samples. Their distinctive characteristics, including localized surface plasmon resonance (LSPR), catalytic, and conductivity capabilities, have an imperative role in the microfluidic signal-transducing platforms. Nobel metal NPs exhibit LSPR, which refers to the phenomenon of light interacting with these NPs and causing a collective oscillation of conduction band electrons.[66] As illustrated in Fig. 1, metal nanoparticles enable sensitive detection in paper-based microfluidic devices via electrochemical, colorimetric, SERS, and chemiluminescent methods by utilizing their plasmonic and catalytic effects. The inter-particle distance of metal NPs plays a crucial role in determining their LSPR, donating them as a valuable diagnostic device for the rapid, cost-effective, and on-site colorimetric detection of various analytes. Given that, a novel colorimetric sensor utilizing metronidazole-stabilized Ag NPs (MTZ-AgNPs) has been developed for the selective, sensitive, and rapid detection of permethrin.[28] The MTZ-AgNPs, which were prepared in yellow color, exhibited a strong LSPR absorbance peak at 400 nm, demonstrating exceptional stability. The introduction of permethrin to MTZ-AgNPs resulted in a change in color to a light-yellow hue as a result of aggregation, and a hyperchromic shift was noted in the LSPR absorbance. To enable the on-site and real-time identification of permethrin, this visual color change is additionally combined with a smartphone and microfluidic paper-based analytical device (μPAD). The colorimetric probe exploiting MTZ-AgNPs demonstrates

Table 1. Comparison of NMs-based microfluidic sensors for various analytes in the food and environmental samples

Technique	Structure	NMs	Target	Reale sample	Linear range	LOD	Ref.
Colorimetric	MTZ-AgNPs	AgNPs	Permethrin	Tomato and apple	0.1 – 50 µM	0.0104 µM	[28]
Colorimetric	Pyrrolidine-1-dithiocarboxylic acid ammonium salt-AgNPs	AgNPs	Al^{3+}, and Cr^{3+}	River water	0.1 – 220 µM, and 0.01 – 250 µM	10.66 nM, and 3.55 nM	[29]
–	Stir-bar functionalized with AuNPs-labeled aptamer	AuNPs	Kanamycin, and chloramphenicol	Milk, and fish	0.001 – 40 ng mL^{-1}	0.52 pg mL^{-1}, and 0.41 pg mL^{-1}	[30]
Colorimetric	Paper strip-monoclonal antibody tagged with colloidal AuNPs	AuNPs	Clarithromycin, erythromycin, roxithromycin, and azithromycin	Milk	–	0.095 ng mL^{-1}, 0.085 ng mL^{-1}, 0.055 ng mL^{-1}, and 0.175 ng mL^{-1}	[31]
Chemiluminescence	AuNPs-aptamer	AuNPs	Sulfadimethoxine	Water	0.01 – 1000 ng mL^{-1}	0.004 ng mL^{-1}	[32]
SERS	AuNPs-target antigen-antibody	AuNPs	MBA, and DSNB	Egg white, cheese, and packaged Juice	10 - 10^7 cells mL^{-1}	100 cells mL^{-1}, and 10 cells mL^{-1}	[33]
SERS	Bipyramid AuNPs	AuNPs	Methyl parathion	Apples, tomatoes, and cucumbers	–	98.63 ng cm^{-2}, 31.56 ng cm^{-2}, and 36.58 ng cm^{-2}	[34]
SERS	Cu based microfluidic channel-Ag NPs	AgNPs	Hg^{2+}	Aqueous solution	1 nM – 1 mM	0.1 µM	[35]
SERS	I^--functionalized AgNPs	AgNPs	Hg^{2+}	Tap water, and lake water	1 nM – 0.1 pM	1 fM	[36]
Fluorescence	Fe_3O_4-AuNPs-dsDNA	MNPs, and AuNPs	17β-estradiol, kanamycin, and Pb^{2+}	Milk, fish, and pork	0.589 pM – 10 nM, 0.394 pM – 3.5 nM, and 0.429 pM – 3.5 nM	0.176 pM, 0.118 pM, and 0.129 pM	[37]
Colorimetric	Fe_3O_4@Au-PS-RNA	MNPs, and AuNPs	Hg^{2+}	Lake water	10 nM – 1 µM	21.9 nM	[38]
Fluorescence	Fe_3O_4@AuNPs-C12SH	MNPs, and AuNPs	Kanamycin, streptomycin, gentamicin, and neomycin	Milk, chicken, and pork muscles	0.03 – 1000 µM, 0.04 – 1000 µM, 0.05 – 1000 µM, and 0.03 – 1000 µM	8.7 nM, 0.012 µM, 0.014 µM, and 0.008 µM	[39]
Fluorescence	Paper@QDs@MIPs	QDs	2,4-D	Soybean sprouts, and mung bean sprout	0.83 – 100 µM	0.12 µM	[40]
Fluorescence	Paper@ZnSe QDs@ ion imprinted polymers	QDs	Cd^{2+}, and Pb^{2+}	Lake water, and seawater	1 – 70 µg L^{-1}, and 1 – 60 µg L^{-1}	0.245 µg L^{-1}, and 0.335 µg L^{-1}	[41]
Colorimetric	GQD-MPA	GQDs	Cu, Fe, Hg, Co, manganese, chrome, and Ni	Water	–	–	[42]
Fluorescence	M-GQDs	GQDs	DOX, pefloxacin, and levofloxacin	Milk, tap water and meat leachate	5 – 50 µM, and 3 – 30 µM	39.30 nM, 48.60 nM, and 35.10 nM	[43]
Fluorescence	Dual-emission CDs	CDs	Parathion-methyl, and glyphosate	Apple, grape, cucumber, tomato, Fructus	0.3 – 65 µM, and 1 – 110 µM	0.14 µM, and 0.6 µM	[44]
Fluorescence	rCDs	CDs	DDVP	Spinach, and tomato	2.5 – 120 µg L^{-1}	1 µg L^{-1}	[45]
Fluorescence	Combining the N-doped CDs with a enzymatic cascade	CDs	Cefquinome	Milk	0.013 – 1.52 ng mL^{-1}	0.78 ng mL^{-1}	[46]
Fluorescence	N, Cu-CDs	CDs	DOX, TC, CTC, OTC, and QCT	Milk, tap water and waste water	–	28.8 nM, 37.2 nM, 23.8 nM, 43.8 nM, 59.3 nM	[47]

Table 1. Continued.

Technique	Structure	NMs	Target	Reale sample	Linear range	LOD	Ref.
Fluorescence	CD-aptamer-MoS_2	CDs	CAP, OTC, and SMZ	Shrimp	0.5 – 100 ng mL^{-1}	0.47 ng mL^{-1}, 0.48 ng mL^{-1}, and 0.34 ng mL^{-1}	48
Fluorescence	N, S co-coped CDs	CDs	Cd^{2+}	Tap water, river water	0 – 2.67 µM	0.705 nM	49
Fluorescence	CDs	CDs	AA	–	0 – 125 µM	2.71 µM	50
–	Single layer graphene FET	Graphene	Chlorpyrifos	–	1 fM – 1 µM	1.8 fM	51
Colorimetric	AChE/GQDs-AuNPs	GQDs, and AuNPs	Chlorpyrifos	Cucumber, lettuce, tomato, and carrot	0.001 – 1 µg mL^{-1}	0.0007 µg mL^{-1}	52
Amperometry	GO	GO	CBF, and CBR	Water, cucumber, and cabbage	0.1 – 2 mg L^{-1}, 0.5 – 7.5 mg L^{-1}	0.06 mg L^{-1}, and 0.4 mg L^{-1}	53
Fluorescence	SPE-GOQD-aptamer	GOQD	As^{3+}, Cd^{2+}, and Pb^{2+}	Lake water	0.01 – 100 µM	5.03 nM, 41.1 nM, and 4.44 nM	54
voltametric	Ag NPs/rGO/flower-like $Ni(OH)_2$/NF	AgNPs, and rGO	Pb^{2+}	River, and Fish	0.01 – 2100 µg L^{-1}	0.00464 µg L^{-1}	55
Fluorescence	MoS_2 QDs-Eu^{3+}	MoS_2 QDs	TC	Tap water, and river water	10 nM – 60 µM	2 nM	56
Fluorescence	N-doped MoS_2 QDs	MoS_2 QDs	Fe^{3+}, and AA	–	20 – 140 µM, and 1 – 100 µM	11 µM, and 960 nM	57
Colorimetric	ZIF-8@paper µPAD	MOFs	Total phenolic compounds	Apple, blueberry, grapes, lemon, pear, strawberry	1.6 – 30 mg L^{-1}	0.5 mg L^{-1}	58
voltametric	AChE/MOF/µE	MOFs	Chlorpyrifos	Cucumber, capsicum, and brinjal	10 – 100 ng L^{-1}	6 ng L^{-1}	59
voltametric	MCH/dsDNA/Au/ MOF-based bio-bar code/SPCE	MOF, and AuNPs	Streptomycin	Milk	0.005 – 150 ng mL^{-1}	2.6 pg mL^{-1}	60
voltametric	MIP/Fe_3O_4/C-dots@ Ag-MOFs	MOFs, Fe_3O_4, and C-dots	Parathion-methyl	Chinese cabbage, banana, apple, water, soil	50 pM – 20 nM	11.6 pM	61
Voltametric	JNU-3@AAO	COF	Hg(II)	Tap water, river water, lake water, and rice	0.01 – 100 pg mL^{-1}	3.28 fg mL^{-1}	62

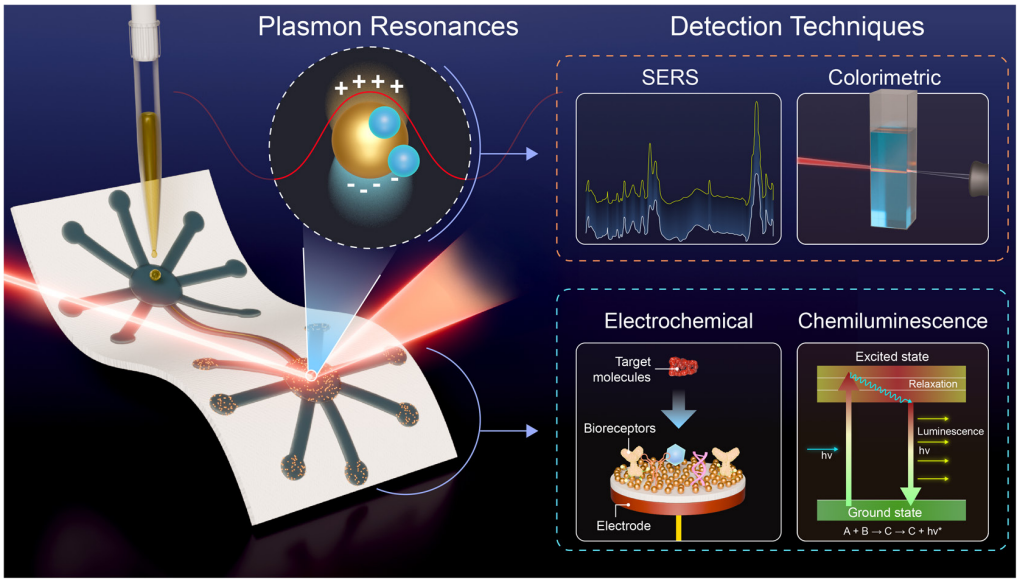

Fig. 1. Sensitive detection in paper-based microfluidic systems is achieved using metal nanoparticles via SERS, colorimetric, electrochemical, and chemiluminescent methods, driven by their plasmonic and catalytic effects. Reprinted from Venugopalan et al[65] under Creative Commons Attribution-NonCommercial (CC BY-NC 3.0) license.

a limit of quantitation (LOQ) of 0.0348 μM and a limit of detection (LOD) of 0.0104 μM. The developed MTZ-AgNPs were effectively used for the colorimetric detection of permethrin pesticide in actual samples. A portable microchip-derived colorimetric probe was reported for the quantification of aluminum ion (Al^{3+}) and chromium ion (Cr^{3+}).[29] The AgNPs were first-time modified with a novel ligand, pyrrolidine-1-dithiocarboxylic acid ammonium salt. The hue of the AgNPs in the testing area promptly shifts upon the introduction of Al^{3+} and Cr^{3+}. The color changes were identified either by the naked eye or by capturing them using a smartphone camera. The acquired images were examined using red, green, and blue (RGB) software to measure the concentration of Cr^{3+} and Al^{3+}. In the case of the μ-chip, the concentration ranges for Al^{3+} and Cr^{3+} are 0.01-220 μM and 0.1-200 μM, respectively, with LOD of 2.30 and 9.18 nM. The μ-chip demonstrated significant promise as a rapid sensing substrate for tracking Cr^{3+} and Al^{3+} in river water samples.

AuNPs have also been widely integrated into microfluidic biosensors due to their excellent catalytic activity, conductivity, and ease of bioconjugation with aptamers, antibodies, and nucleic acids. In one representative study, Zhang's group reported microfluidic microchip electrophoresis using an aptasensor for the determination of kanamycin and chloramphenicol (CAP) in fish and milk samples.[30] The probe engaged a stir bar coupled with AuNPs to simplify deoxyribonucleic acid (DNA) multi-arm junctions recycling (MAJR) for signal amplification and transduction aims. During the diagnosis procedure, the antibiotics were precisely coupled with a specific aptamer on the stir bar to generate diverse sole-tagged DNA primers. The primers then induced the MAJR procedure to link the four-arm and three-arm DNA of the various analytes. Lastly, the multi-arm DNA is successfully detached through MCE for quantitative determination. It is revealed that the device realized LODs of 0.41 and 0.52 pg mL^{-1} for kanamycin, and CAP, respectively. This study elucidated the robust amplification potential of gold nanoparticle-facilitated nucleic acid engineering in microfluidic platforms.

Similarly, AuNP-labeled immunochromatographic paper-based microfluidic systems have shown high applicability for multiplex antibiotic detection. Zeng et al established a microfluidic lab-on-paper probe for the quick identification of four macrolides i.e. azithromycin, roxithromycin, erythromycin, and clarithromycin in milk samples.[31] In the sensing procedure, anti-mouse-goat IgG antibodies and antigens were primarily immobilized on the safety paper strip as test line and control line. Then, a monoclonal antibody is tagged with colloidal Au, and a sample solution is introduced to induce the antibiotics to bind with the monoclonal antibody. Lastly, the mixed solution containing the monoclonal antibodies and the target antibodies was released onto the earlier-formed immune paper strip. The monoclonal antibodies labeled with colloidal Au and antibodies were then subjected to a competitive binding with the immunochromatographic strip to generate a color alteration. The proposed microfluidic chip can detect azithromycin, roxithromycin, erythromycin, and clarithromycin, in milk samples with LODs of 0.175, 0.055, 0.085, and 0.095 ng mL^{-1}, respectively. Unlike traditional ELISA methods, these AuNP-based paper microfluidic systems meaningfully improve portability and reduce assay time. Nevertheless, antibody-based recognition systems still encounter limitations in terms of limited shelf life, biomolecule instability, and susceptibility to storage and temperature conditions.

In addition to colorimetric sensing, AuNPs have been widely explored in chemiluminescence-based microfluidic systems because of their catalytic enhancement capability. For example, luminol-catalyzed chemiluminescence, enhanced through AuNP aggregation, has been utilized for the detection of sulfadimethoxine within an aptamer-based microfluidic flow-injection system (Fig. 2).[32] Importantly, the investigation revealed that effective fluid mixing plays a pivotal role in determining sensor performance, with a five-layer 3D microfluidic mixer exhibiting markedly superior results compared to traditional 2D designs. This outcome underscores a critical yet frequently neglected consideration in the design of microfluidic sensors: that analytical efficacy is influenced not only by the intrinsic properties of NMs but also by the optimization of microchannel architecture and fluid dynamic behavior.

Surface-enhanced Raman spectroscopy (SERS)-based microfluidic systems incorporating AgNPs and AuNPs have also gained considerable attention owing to their molecular fingerprinting capability and ultrahigh sensitivity. AuNP-engineered SERS immunoprobes are effectively used for pesticide and pathogen detection through electromagnetic field enhancement at nanoparticle "hot spots." For example, bipyramidal AuNPs united with portable Raman systems enabled highly sensitive quantification of methyl parathion residues on vegetable and fruit surfaces. The sharp-tip morphology of bipyramidal AuNPs enhanced local electromagnetic fields and significantly improved SERS signal intensity.[34] AgNP-based SERS microfluidic platforms have also shown excellent performance for heavy metal detection. Yan et al reported an in situ electroless galvanic replacement approach for synthesizing Ag nanostructures directly within microfluidic channels for Hg^{2+} sensing.[35] Likewise, iodide-functionalized Ag aggregate substrates enabled rapid "turn-off" SERS detection of Hg^{2+} with response times of around 150 s and a wide detection range of 10^{-9} to 10^{-13} M. These studies highlight the remarkable sensitivity achievable through plasmonic nanostructures; however, long-term operational stability and interference from competing ions remain insufficiently investigated.

Overall, noble metal NP-coupled microfluidic systems have considerably innovative rapid chemical contaminant analysis by merging high sensitivity with miniaturization and portability. Despite significant progress, numerous critical challenges continue to

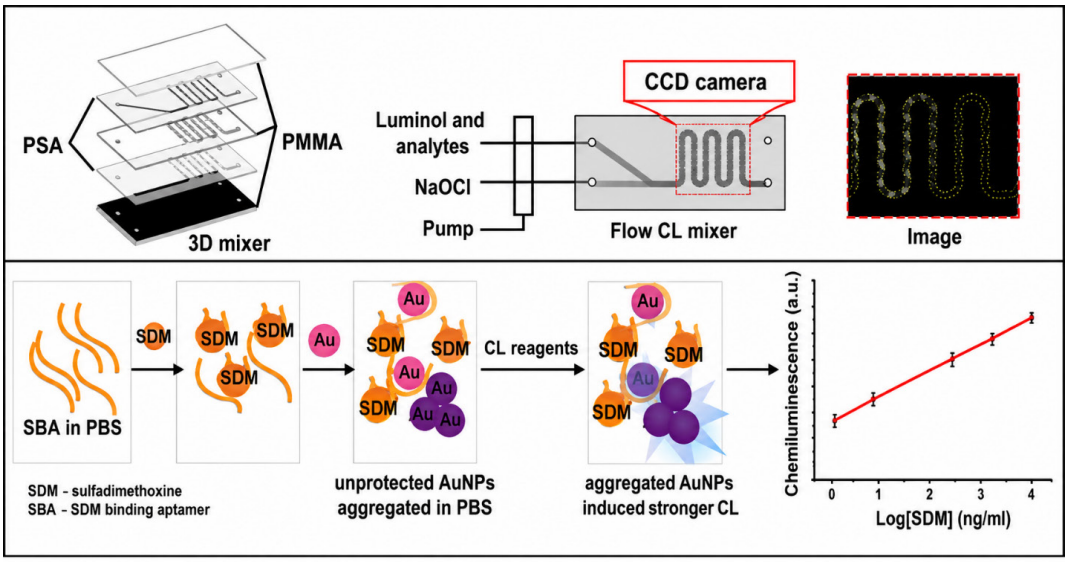

Fig. 2. Schematic representation of the PMMA-based microfluidic chip featuring four integrated 3D mixers and PSA-sealed layers, designed for continuous flow-injection chemiluminescence detection of sulfadimethoxine. Reprinted from Wang et al[32] under the Creative Commons Attribution 4.0 International License (https://creativecommons.org/licenses/by/4.0/).

hinder practical deployment. Most current research mainly concentrates on AgNPs and AuNPs, whereas other metallic NMs, such as Cu-, Pd-, Pt-, and Fe-based nanoparticles, remain insufficiently explored despite their potentially distinctive electrochemical and catalytic characteristics. Furthermore, optical sensing methods dominate the literature, while comparatively limited attention has been directed towards electrochemical, electrochemiluminescence, photoelectrochemical, and piezoelectric microfluidic sensors that incorporate metallic nanoparticles.

Magnetic NPs

Magnetic NPs refer to NMs exhibiting superparamagnetic characteristics. These particles may consist of magnetic metals such as Fe, cobalt (Co), or nickel (Ni), their oxides like maghemite hematite (g-Fe_2O_3), and magnetite Fe oxide (Fe_3O_4).[67] Iron oxide NPs are frequently used in the field of biomedicine, whereas Ni and Co are prone to oxidation and possess toxic properties.[68] Superparamagnetic NPs display the on-off behavior of magnetization when a magnetic field is present or absent, making them well-suited for targeted separation applications. Recently, the application of MNPs for the detection of diverse analytes in environmental and food samples has garnered the interest of researchers. The synthesis and surface functionalization of MNPs are summarized in Fig. 3.

Current study has increasingly focused on multiplex microfluidic biosensors capable of concurrently sensing multiple types of contaminants that usually coexist in food and environmental samples. In this regard, a magnetically encoded aptamer-based microfluidic system was established for the simultaneous determination of Pb^{2+}, kanamycin, and 17β-estradiol ions.[37] As illustrated in Fig. 4, magnetic bead (MB)-double-stranded DNA (dsDNA) conjugates were exploited for signal amplification and conversion. The detection procedure was based on a multibranched hybridization chain reaction (mHCR), which produced multi-branched DNA nanostructures exhibiting improved amplification efficiency and specificity. Importantly, magnetic separation minimized matrix interference from complex food samples and enhanced diagnostic reliability. The platform achieved ultralow LODs of LOD of 1.76×10^{-4} nM for kanamycin, 1.18×10^{-4} nM for 17β-estradiol, and 1.29×10^{-4} nM for Pb^{2+}, indicating the excellent sensitivity achievable through magnetic-assisted nucleic acid amplification approaches. This study highlights some important benefits of MNP-based microfluidics, like efficient target enrichment, compatibility with multiplex analysis, and reduced nonspecific interference. Nevertheless, the system also proves current constrains associated with nucleic acid amplification-based sensing, such as relatively high assay costs, increased operational complexity, and complicated probe design.

Magnetic manipulation approaches have also revealed important potential for visual and portable heavy metal detecting.

A valuable work reported a microfluidic magnetic manipulation system exploiting Au-coated MNPs and phosphorothioate-ribonucleic acid (PS-RNA) probes for visual analysis of Hg^{2+}.[38] In this system, PS-RNA probes were anchored onto Au-coated MNPs through Au–S and biotin-avidin bindings and subsequently integrated with polystyrene microspheres to create a self-assembled configuration known as a MAPP bead. In the Hg^{2+}presence, PS-RNA cleavage induced departure of the polymeric and magnetic elements. Following MNPs magnetic removal, cleaved microspheres accumulated within a particle trap, generating a visible strip whose length associated with Hg^{2+} amount. The platform exhibited a LOD of 21.9 nM with high selectivity for Hg^{2+}. However, the sensitivity of this assay is comparatively

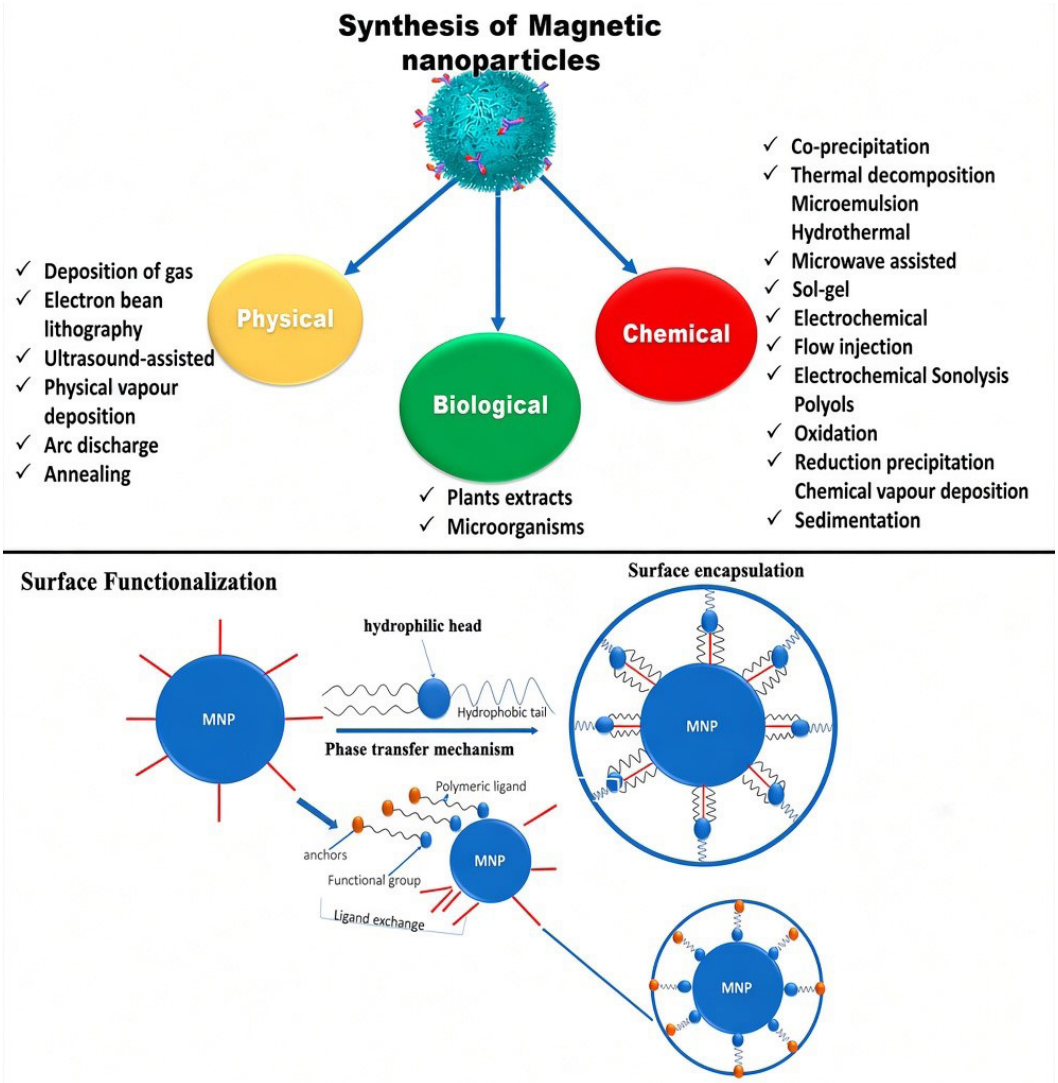

Fig. 3. Schematic representation of the synthesis approaches for magnetic nanoparticles and the surface functionalization mechanisms, including phase transfer and ligand exchange. Reprinted from Adeeyo et al[67] under the Creative Commons Attribution (CC BY) license (https://creativecommons.org/licenses/by/4.0/).

lower than that achieved by more sophisticated optical or SERS-based methodologies, suggesting an inherent compromise between ease of operation and analytical sensitivity. Furthermore, reliance on nucleic acid cleavage mechanisms may constrain the assay's robustness when subjected to fluctuating environmental conditions.

Beyond magnetic separation, MNPs have also been combined into localized sensing zones within microfluidic devices to improve signal generation and analyte capture efficiency. Magnetic materials activated with aptamers, enzymes, antibodies, or encapsulated reagents can be selectively retained in sensing chambers using external magnetic fields, thereby minimizing analyte loss and improving reaction localization. In this regard, hybrid magnetoliposomes (h-MLs) containing hydrophobic Fe_3O_4@AuNPs-C12SH nanoparticles and encapsulated N-acetylcysteine were used for sensing aminoglycoside antibiotics, including streptomycin, kanamycin, neomycin, and gentamicin.[39] In this system, magnetoliposomes activated simultaneously as reagent concentrators and magnetic carriers within the microfluidic detection region. The interaction with o-phthalaldehyde resulted in the formation of fluorescent isoindole derivatives, yielding signals that correlated directly with the analyte concentration. This approach exemplifies the multifunctional potential of MNP-based systems, wherein magnetic enrichment, reagent delivery, and signal amplification are seamlessly integrated into a unified platform. Nonetheless, the synthesis of hybrid magnetoliposomes is comparatively intricate and may pose challenges regarding scalability for mass production and commercial application.

The existing microfluidic sensor landscape, especially those utilizing MNPs, demonstrates an important deficiency in analyte identity in environmental and food samples, mostly concentrating on optical methods such as fluorescence and colorimetric sensors. The restricted scope underscores the necessity for a more extensive range of methods for identification to effectively leverage the distinctive characteristics of MNPs. Subsequent investigations ought to examine alternate techniques, including electrochemical, electrochemiluminescence,

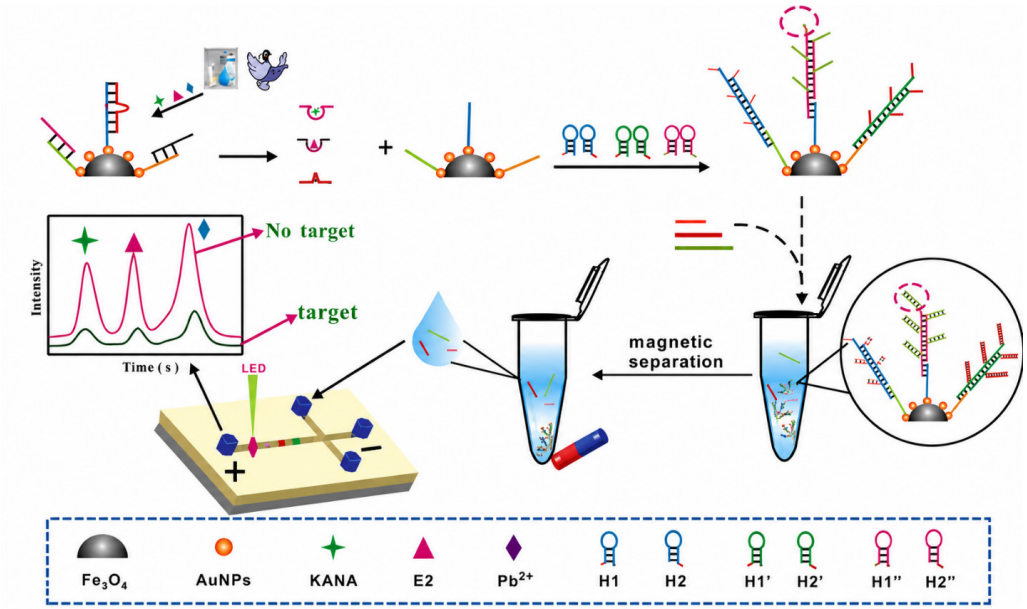

Fig. 4. The process of identifying various chemical contaminants involves the integration of an aptamer sensor with hybrid chain reaction amplification within a microfluidic platform. Reprinted with permission from Chen et al.[37] Copyright 2026 American Chemical Society.

and photoelectrochemical sensors employing MNPs, which may provide improved sensitivity and specificity. Researchers should concentrate on optimizing microfluidic system designs to improve fluid manipulation and analyte capture efficiencies, integrating multi-modal sensing platforms that amalgamate diverse detection techniques, and establishing standardized protocols to ensure reproducibility and facilitate comparative evaluations across studies. Implementing these tactics will improve the functioning and effectiveness of MNP-based sensors, hence augmenting their contributions to environmental monitoring and food safety evaluations.

Quantum dots

Quantum dots (QDs) are semiconductor nanocrystals with excellent optical and electronic features because of their nanometer-sized diameters.[69] QDs could contribute to biosensor construction in two ways: by providing signal amplification and by modifying the sensor screen. Within microfluidic systems, QDs mainly function as signal amplification elements, fluorescent signal transducers, or surface-modification materials to enhance diagnostic sensitivity and multiplexing ability.

Among various QDs, cadmium telluride (CdTe) QDs have been broadly explored owing to their outstanding fluorescence function and facile synthesis. Zhang's group reported a new paper@QDs@molecularly imprinted polymers (MIPs) fluorescent probe toward 2,4-dichlorophenoxyacetic acid (2,4-D) using electron-transfer-triggered fluorescence quenching procedure.[40] The detecting procedure relied on electron-transfer-induced fluorescence quenching between the imprinted QD structure and the analyte. The resulting system displayed a low LOD of 0.12 μM with low analysis time 18 min, while preserving low cost, portability, and simple post-processing necessities. Despite the superior analytical capabilities of CdTe QDs, concerns regarding their environmental and biological safety persist and warrant comprehensive further investigation.

To mitigate toxicity issues related to cadmium-based quantum dots, research has focused on alternative semiconductor NMs that exhibit enhanced biocompatibility. For example, a zinc selenide (ZnSe) QDs were successfully synthesized using ion imprinting technology and incorporated into 3D rotary μPADs. This innovative approach enables the selective and simultaneous determination of cadmium ion (Cd^{2+}) and Pb^{2+}.[41] In contrast to CdTe QDs, ZnSe QDs are characterized by lower toxicity and greater environmental friendliness. Furthermore, this innovation has enhanced the device's portability by converting the liquid phase of ZnSe QDs@ion imprinted polymers to solid glass fiber paper. The shift from liquid-phase to solid-state sensing constitutes a significant progression in the development of field-deployable microfluidic systems. Nevertheless, ion-imprinting methodologies may continue to encounter challenges related to suboptimal binding kinetics and incomplete removal of template ions, which could adversely impact both selectivity and reproducibility. Furthermore, the long-term fluorescence stability of ZnSe QDs under diverse environmental conditions has not been comprehensively investigated.

In contrast to conventional quantum dots composed of heavy metals, graphene quantum dots (GQDs) provide environmentally benign sensing platforms while preserving robust fluorescence characteristics. The fluorescence behavior of GQDs can be modulated via interactions with metal ions, leading to either fluorescence enhancement or quenching phenomena, which are advantageous for the sensitive detection of analytes. In this context, Abdollahian et al outlined the production

of different thiolated-GQDs to enable the simultaneous multi-sensing of heavy metal ions through one-droplet OD-μPADs.[42] Functionalized GQDs were successfully synthesized and immobilized on hydrophobic fiberglass using a straightforward manufacturing and assembly approach. This method enables the colorimetric detection of various ions such as Cu, Fe, Hg, Co, manganese, chrome, and Ni. To achieve this objective, GQDs are modified with different organic compounds like mercaptopropionic acid (MPA), decanethiol, and cysteamine to facilitate targeted electrostatic interactions with metal ions. Ultimately, this efficient and simple colorimetric platform was employed to easily detect metal ions in simulated environmental fluids and human urine. This technology has the potential to be developed into a commercial device for identifying contaminants by individuals without professional expertise in environmental and biomedical fields.

Recent studies have also focused on heteroatom-doped GQDs to improve fluorescence stability, selectivity, and multifunctionality. In this regard, Qian and colleagues introduced an innovative fluorescent sensor designed to differentiate and track TCs, oxazine-modified fluoroquinolones (OFQs), and alkane-modified fluoroquinolones (AFQs). This sensor is based on multi-doped GQDs (M-GQDs) containing phosphorus, nitrogen (N), and fluorine atoms.[43] The M-GQDs demonstrate robust blue emission at 419.0 nm and exceptional stability, providing a basis for the convenient discrimination and sensitive tracking of TCs, OFQs, and AFQs. Particularly, the fluorescence of M-GQDs is inhibited by TCs through the process of inner filter effect (IFE). Additionally, the presence of AFQs leads to a redshift and amplification of M-GQDs fluorescence, attributed to constrained conformational rotation facilitated by hydrogen bonding, π-π stacking, and electrostatic interactions. In the meantime, the oxazine ring's electron-accepting characteristic in oxazine-modified OFQs enhances the emission peak at 498.0 nm and diminishes the emission peak at 419.0 nm, resulting in a shift in color from blue to cyan. However, the introduction of OFQs results in the observation of dual emission peaks, which is ascribed to electron transfer (ET) induced by the presence of oxazine rings in the structural composition.

Carbon dot (CDs)

Carbon dots -based fluorescent platforms have fascinated more considerations to screen pesticide residues with exceptional low LOD, high sensitivity, tunable emission, and photo-stability.[70] In this regard, a dual-emission CDs-centered nonenzymatic fluorescent scaffold is designed, which displays exceptional selectivity and sensitivity in simultaneously sensing glyphosate and parathion-methyl.[71] Carbon dots with emissions at 660 nm red emission CDs (rCDs) and 440 nm blue emission CDs (bCDs) are created through hydrothermal treatment of sodium hydroxide and mulberry leaves. Blue emission CDs react to hydrolyzed parathion-methyl through an internal filter effect, whereas rCDs detect glyphosate with the help of Cu^{2+}upon static quenching influence. Good linear ranges were found for glyphosate (1.0-110.0 μM) and parathion-methyl (0.3-65.0 μM) with LOD at 0.14 and 0.60 μM. Additionally, ratiometric system association with facile substrates like smartphones, and μPADs would be favorable for visual and on-site pesticide identification.[72] 3D μPADs are well-matched with chemiluminescent and electrochemistry nanoprobes for the quantification of pesticide residues, and the amalgamation of fluorometry sensors and 3D μPADs is promising for analysis. In this context, a ratiometric fluorescent tactic incorporating threaded 3D μPAD was initially advanced for organophosphorus pesticide diagnosis in agricultural samples.[45] Via solvothermal treatment of cilantro, rCDs were produced. Dichlorvos (DDVP), a common organophosphorus, precisely suppressed butyrylcholinesterase function to generate cascade responses in the sensing system. As the concentration of DDVP increased, the fluorescent 3D μPAD images visually ranged from red to yellow. In actual sample analysis, threaded 3D μPAD successfully inhibited the sample pigments interference for organophosphorus determination. The fluorescent images offered distinct color variations with pesticide concentrations ranging from 2.5 to 120 μg L^{-1} and LOD of 1.0 μg L^{-1}. The brilliant performance of 3D μPAD delivered a background-free, instrument-free, and accurate substrate toward organophosphorus and showed great potential in environmental, and food safety monitoring grounds. More recently, by combining the CDs with a well-developed enzymatic cascade enhancement platform, an IFE -derived fluorescence immunoprobe is designed for highly sensitive detection of cefquinome in milk samples.[46] In this work, the N-doped CDs are constantly manufactured through a simple microfluidic approach at 90 °C, and their quantum yields achieved 19.2%. The properties of the gained CDs can be monitored in real time in order to synthesize CDs with particular features. The fabricated fluorescence immunoprobe delivered a low LOD of 0.78 ng mL^{-1}, which satisfied the maximum residue limit established via authorities. This probe shows a good linear range of 0.013-1.52 ng mL^{-1} with an 50% inhibition concentration of 0.19 ng mL^{-1} against cefquinome. In comparison with classical techniques, the microfluidic probe was further flexible on CDs and the designed fluorescence scaffold was eco-friendlier and highly sensitive toward ultra-trace cefquinome residue exploration. In another example, Li et al reported a 3D ratiometric fluorescence probe using the Cu and N co-doped CDs (N, Cu-CDs) for effectively sensing quercetin (QCT) and tetracyclines (TCs).[47] The N and Cu-CDs are made from anhydrous Cu chloride and ethylene diamine tetraacetic acid (EDTA) as precursors by hydrothermal procedure and show bright blue fluorescence with brilliant optical stability. Upon the existence of the chlortetracycline (CTC), TC, doxycycline (DOX), and oxytetracycline (OTC), the N, Cu-CDs fluorescence intensity was directly quenched owing to the internal filtration influence, and the LOD found upon sole-signal

fluorescence identifying is as low as 28.8 nM for CTC, 37.2 nM for TC, 23.8 nM for DOX, and 43.8 nM for OTC. Considerably, a 3D ratiometric fluorescence system for sensing QCT is suggested using the presence of another emission at (490 nm and 410 nm) as a result of the electron transform procedure. This newfangled technique displays a low LOD of 59.3 nM with a broad linear range of 10-100 μM. Additionally, a dual-channel fluorescence detecting scaffold using μPADs is successfully advanced for simultaneous on-site discrimination of TCs and QCT. Tong's group introduced a laser-printed μPADs chip charged with multicolor fluorescence systems to quickly determine CAP, OTC, and sulfamethazine (SMZ).[48] These "fluorescence off" identification systems assembled using CDs integrated with molybdenum disulfide (MoS_2) nanosheets (acceptor) and aptamers (donor) (CD-apt-MoS_2) are according to Förster resonance energy transfer. After the target antibiotics were added, the fluorescence response in the μPAD could be meaningfully detected using a 3D-printed portable identification box via a smartphone. This μPAD enabled a fast reaction (15 min) for CAP, OTC, and SMZ with significant sensitivities of 0.34, 0.48, and 0.47 ng mL^{-1}, respectively. To sum up, this paper-based probe can be provided new horizon for high-throughput, on-site, and rapid recognition approaches and would be broadly utilized in point-of-care-testing (POCT) in food safety.

Despite the increasing attention towards CDs for their potential applications as nanosensor, the reproducible and rapid synthesis of CDs remains a critical challenge for achieving scalable production and practical utilization. The microreactor system was utilized to continuously produce functionalized CDs with a high degree of uniformity. Sulfur and N co-doped CDs were synthesized from citric acid and L-cysteine using a coiled microreactor within a 10-minute. The resulting N, S co-coped CDs displayed a nearly spherical shape with an average diameter of 2.8 nm and demonstrated intense blue fluorescence when stimulated by ultraviolet light, achieving a notable quantum yield of 68.2%. The fluorescence was able to be specifically suppressed by Cd^{2+} and was proven to be well-suited for the sensitive and highly selective detection of Cd^{2+}. The N, S co-doped CDs achieved a LOD of 0.705 nM over a broad linear range from 0 to 2.67 μM.[49] Environmental and instrumental fluctuations are common reasons for error in smartphone-based microfluidic systems, meaningfully impacting the precision of diagnostic measurements. In this context, spotting the reference and sample concurrently and in close proximity compensates for the fluctuations. The "dual-spot" design bears resemblance to the double-beam method engaged in spectrophotometry, aiming to minimize fluctuations in the outcomes. The fundamental assumption is that any factors affecting the color intensity in the detection zones, whether instrumental or environmental, will have a similar effect on the color intensity in the control zone under the same conditions. Herein, a ratiometric μPAD, functionalized with a mixture of red-emissive ethidium bromide and green-emissive CDs, was established for the selective determination of the analyte.[50] The fluorescence produced by the CDs is suppressed by both Fe^{3+} and ascorbic acid (AA); therefore, NaF was incorporated into the 3D connector as a masking agent to eliminate the disruptive influence of the Fe^{3+} ions. The color changes were observed under an ultraviolet (UV) lamp, with images captured using a smartphone, and the RGB intensities were analyzed using the Color Grab application. The suggested dual-spot technique significantly improved the device's analytical precision and accuracy. It resulted in a linear working range of 0 to 125 μM and a LOD of 2.71 μM.

Polymeric nanomaterials

Polymeric nanomaterials are another fascinating 0D NMs in microfluidic sensing systems owing to their chemical stability, mechanical flexibility, ease of functionalization, and remarkable biocompatibility. A variety of polymer-based nanomaterials, such as conductive polymer nanocomposites, molecularly imprinted polymers (MIPs), polymer NPs, and dendrimers, have been integrated into microfluidic platforms, enabling the sensitive determination of chemical contaminants. Therefore, the selectivity of analytes and signal transduction could be enhanced, and stable immobilization sites for recognition elements and biomolecules could be formed.[73] Notably, MIP-based polymeric nanomaterials have been widely employed in microfluidic sensors for the selective identification of antibiotics, pesticides, and other harmful compounds in environmental and food samples. For example, a QDs-based molecularly imprinted fluorescence sensor (QDs@MIPs) integrated with an inertial microfluidic separation device was developed for the rapid determination of enrofloxacin in contaminated food samples.[74] In this system, QDs@MIPs with a size of micron enabled sensitive and selective recognition, whereas the particle separation is efficiently enabled by a spiral microfluidic channel. The platform achieved a low LOD of 0.059 μg mL^{-1} and a high separation efficiency of 97.7% for enrofloxacin. This research emphasizes the potential of polymeric NMs to combine sample separation, pretreatment, and determination into a unified microfluidic platform for the rapid analysis of food contaminants. Furthermore, a chromatographic paper-mantled 3D-printed microfluidic hybrid device was fabricated for the swift colorimetric detection of As^{3+} utilizing very minimal sample volumes.[75] Here, arsine gas produced in situ interacts with Ag(I) ions that are immobilized on the paper detection zone, resulting in the formation of dark brown silver arsenide, sensitive and selective detection of arsenic. The platform demonstrated a low LOD of 3 μg L^{-1} in a linear detection range of 100-1000 μg L^{-1}. Moreover, it displayed excellent selectivity against other metal ions. This work further highlights the profits of paper-based materials combination with microfluidic architectures to form cost-effective and portable sensing systems.

Two-dimensional NMs

Two-dimensional NMs consist of thin layers that can be as thin as a single atomic layer and extend in two dimensions, indicating that two dimensions of the 2D NM are beyond the nanoscale (greater than 100 nm). The material contains nanoflake, nanosheet, nanoplate, and nanolayers. Owing to their great specific surface area, modifiability, and attractive chemical and physical features, 2D NMs have garnered growing interest and attention from different scientific grounds, including microfluidic platforms.[15] Among these materials, graphene, reduced graphene oxide)rGO(, graphene oxide)GO(, and are commonly employed in microfluidic systems, while other materials such as Au@graphitic carbon nitride (g-C_3N_4) nanosheet and MoS_2 nanosheet are also exploited due to their distinctive properties and advantages.[76]

Graphene oxide

GO has sparked significant scientific interest in (bio)sensing utilizations thanks to its excellent fluorescence quenching ability, wide contact area, good water dispersibility, biocompatibility, tunable chemical and physical characteristics, and ease of surface modification.[77,78] Numerous researchers have employed GO materials like rGO. The investigators explored the impact of different DNA nanoprobe attachment techniques on the sensitivity of rGO transistors. This included long capture tests using π-π stacking interaction, short capture tests using π-π stacking interaction, and covalent immobilization through a linker. Based on research findings, the rGO transistor performed well in terms of sensitivity and stability during the extended capture test.[79] Microfluidic mixing is utilized to coat GO nanoflakes with cationic lipids for gene delivery. Single lipids and GO layers are blended in a regulated microfluidic environment and found to form homogeneous nanohybrid composites with surface charge and appropriate size.[80]

Mechanical exfoliation remains one of the most widely adopted methods for producing highly ordered graphene structures for sensing applications.[51] Graphene exfoliated on 285nm thick silicon dioxide (SiO_2) using based on the scotch tape method. Then, it was employed to construct a microfluidic-derived graphene field effect transistors (FET) platform based on the Cr/AuNS as source-drain chips and e-beam lithography. The graphene on the established FET was engineered via 1-ethyl-3-(3-dimethylaminopropyl) carbodiimide (EDC)/N-hydroxysuccinimide (NHS) to anchor anti-chlorpyrifos on its interface for the chlorpyrifos detecting (an organophosphate (OP) insecticide) (Fig. 5). The construction of a FET-derive probe upon graphene was also operative enough to determine chlorpyrifos through exploring immunoreactions. The graphene FET exhibited can detect chlorpyrifos with a LOD of 1.8 fM and a linear range of 1 fM -1 μM.

In another study, Chungchai et al reported a novel 3D-μPAD for colorimetric determination of chlorpyrifos based on the GQD capped Au nanostructures (AuNPs-GQDs).[52] The 3D-μPAD was constructed through a one-step polymer-screen-printing procedure, without requiring baking or heating the device. The simple production technique provides a foldable tool that contains both sampling and testing sheets. Acetylcholinesterase enzyme-catalyzed hydrolysis of ATCh yields thiocholine, which then binds with aggregated AuNPs-GQDs. The colorimetric examination relies on the hue alteration that happens in AuNPs-GQDs upon binding with thiocholine. Au NPs are synthesized through GQDs as capping and reducing agents. This probe could identify chlorpyrifos via ImageJ diagnosis with a LOD of 0.0007 μg mL^{-1} and a linear range of 0.001-1.0 μg mL^{-1}. The designed 3D-μPAD can sense chlorpyrifos with percent recoveries ranging from 93.0 to 104.6% and RSD ranges of 0.3 - 1.6 in vegetable samples. More recently, Kunpatee's group introduced an electrochemical paper-centered tool for the real-time separation and simultaneous detection of carbaryl (CBR) and carbofuran (CBF).[53] The technology integrated

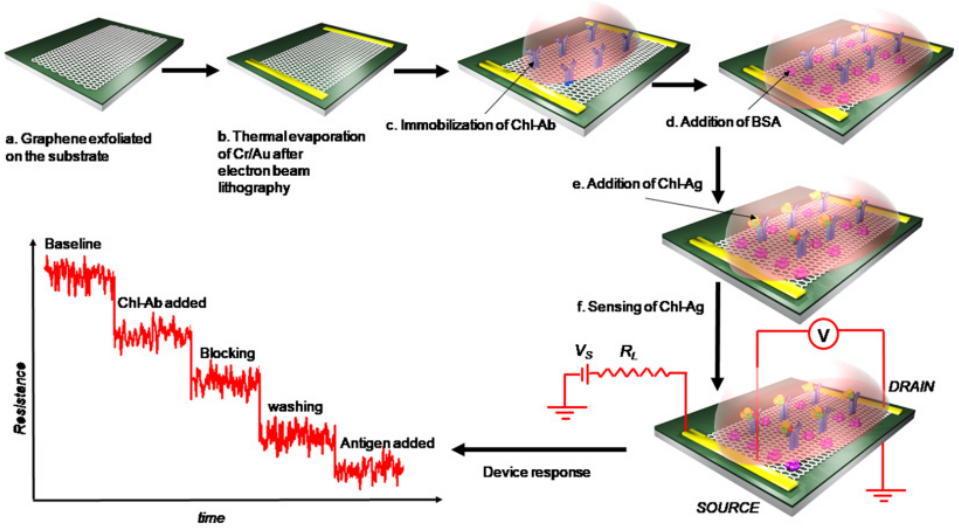

Fig. 5. Mechanically exploited graphene for the fabrication of microfluidic-based graphene probe toward chlorpyrifos sensing. Reprinted from Islam et al[51] under the Creative Commons Attribution 4.0 International License (https://creativecommons.org/licenses/by/4.0/).

an electrochemical sensor and paper chromatography into a sole platform to enhance the detection selectivity of the two pesticides. The two carbamate separations throughout the simultaneous diagnosis of CBR and CBF are recognized based on alterations in the substance's motions on the chromatographic paper in the moving phase flow. The isolated pesticides were confirmed electrochemically using an amperometry technique. The suggested probe affords a linear range for the detection of two pesticides from 0.1 to 2.0 and 0.5-7.5 mg L^{-1}, with LODs of 0.06 and 0.40 mg L^{-1} under optimal conditions, which comprise the influence of the separation channel, mobile phase, and applied potential. Besides, they can effectively identify CBR and CBF in water, cabbage, and cucumber samples. This established electrochemical paper-based device (ePAD) is low-cost and uses a low sample amount. Additionally, it is portable, disposable, and a hopeful device for real-time pesticide screening in real samples.

In order to enhance the sensitivity and specificity of microfluidic sensing systems, there has been a growing incorporation of functional NMs into sensor platforms. This integration is attributed to the distinctive physicochemical properties of these NMs, such as their elevated catalytic activity, superior capacity for biomolecule immobilization, and accelerated electron-transfer (ET) dynamics. Among these, rGO stands out as a highly desirable material due to its exceptional electrical conductivity, strong chemical stability, and significant specific surface area, rendering it highly attractive in biosensor applications. In this study, a composite Ag NPs/rGO/flower-like Ni hydroxide ($Ni(OH)_2$) was fabricated on nickel foam (NF) via a straightforward one-step hydrothermal method, notably without employing nickel precursor salts.[55] The three-dimensional porous architecture of the NF, in conjunction with the extensive surface area of rGO and the flower-like morphology of $Ni(OH)_2$, alongside the superior electrical conductivity of AgNPs, collectively contributed to a high density of active sites and facilitated rapid electron-transfer kinetics during electrochemical sensing. These synergistic characteristics markedly improved the signal amplification performance of the sensing platform. The fabricated probe displayed the exceptional capability for screening of Pb^{2+} ranging from 0.01 μg L^{-1} to 2100 μg L^{-1} with a low LOD of 0.00464 μg L^{-1}. Additionally, this mobile device has been effectively showcased for the identification of Pb^{2+} (ranging from 0.01 μg L^{-1} to 2100 μg L^{-1}) in river water (LOD = 0.00498 μg L^{-1}), and fish (LOD = 0.00566 μg L^{-1}).

Other 2D nanomaterials

In recent years, transition metal dichalcogenides (TMDs) have emerged as an important class of 2D NMs for biosensing and microfluidic applications.[81] Transition metal dichalcogenides share similarities with graphene but exhibit lower thinness and mechanical strength while demonstrating superior electrical conductivity due to their direct gap band structure.

Among the various TMDs, MoS_2 has been the most broadly explored in microfluidic systems owing to its large surface area, excellent electrical conductivity, favorable chemical stability, and tunable optical properties. To further enhance the electrochemical function of MoS_2 nanosheets, nanohybrid composites consisting of metal NP-decorated MoS_2 structures are frequently developed and integrated into microfluidic devices. This approach preserves the unique properties of both MoS_2 nanosheets and metal NPs, while also introducing novel attributes arising from their synergistic combination.[82] In this context, an innovative ratiometric fluorescent assay based on the amalgamation of europium ion (Eu^{3+}) and MoS_2 QDs, expanded the use area of MoS_2 QDs.[56] Ultrafine and uniformly dispersed MoS_2 QDs were successfully synthesized via a straightforward one-step hydrothermal approach. The resulting MoS_2 QDs demonstrated a fluorescence emission peak centered at 470 nm when excited at 400 nm. This particular excitation wavelength was chosen because it produced comparable fluorescence intensities for both Eu^{3+} ions and MoS_2 QDs, thereby facilitating the development of a robust ratiometric fluorescence system. In the existence of MoS_2 QDs, the characteristic emission peak of Eu^{3+} was meaningfully improved, thereby establishing a dual-emission ratiometric sensing mechanism. This approach minimized environmental interference and enhanced analytical accuracy. This probe can detect TC with a LOD of 2 nM and a wide linear range of 10 nM-60 μM.

Most MoS_2 QDs-based probes encounter inherent issues with selectivity and photostability due to the absence of functional modification. Recent studies have indicated that addressing these limitations can be achieved through heteroatom doping, specifically by introducing N or sulfur. This is an effective approach to enhance the characteristics of QDs. Nevertheless, there is a pressing need to develop a N-doped MoS_2 QDs-based sensing system that can operate with high sensitivity in microfluidic logic gates to fulfill the requirement for multi-target sensing. In this context, N-doped MoS_2 QDs were prepared and developed as fluorescent probes for dual-target sensing and microfluidic logic gate operations.[57] By deliberately adjusting the aggregation and dispersion of QDs, N-doped MoS_2 QDs can function as dual-target fluorescence probes with the ability to sequentially detect Fe^{3+} and/or AA through a fluorescence "on-off-on" mechanism. This study examines the fluorescence quenching process between N-doped MoS_2 QDs and Fe^{3+} ions. This dual-target sensor has the potential to serve as a fluorescence logic gate for the visual quantification of Fe^{3+}, AA, and their mixture. In addition, they have developed a microfluidic logic gate by controlling the fluorescence change of N-doped MoS_2 QDs. The consistent large-scale production of high-quality TMD with precise control over thickness, morphology, and defect density continues to present significant challenges. Furthermore, comprehensive studies are necessary to evaluate the long-term stability and potential environmental effects of TMDs under practical operational conditions.

Three-dimensional NMs

3D NMs are materials that extend beyond the nanometric scale and are constructed from low-dimensional nanostructures, such as 0D, 1D, and 2D units. 3D NMs (including covalent organic frameworks (COFs), metal-organic frameworks (MOFs), and nanocomposites with various buildings like nanostars and nanoflowers) have been utilized in microfluidics for the identification of chemical contaminants.[83]

MOFs and COFs

The combination of the μPAD system with MOFs can be a hopeful substitute to construct a nanocomposite taking profit from the simplicity and permeability of capturing the MOF's performance and cellulosic paper.[83,84] One representative example of a MOF-integrated μPAD for the determination of total phenolic compounds in fruit samples.[58] The designed probe was optimized with respect to MOF amount, sample volume, and design. Additionally, to control the correct hybridization, the ZIF-8@paper was characterized in depth based on scanning electron microscopy (SEM), powder X-ray diffraction (p-XRD), and Fourier-transform infrared (FT-IR). Subsequently, the established technique was effectively used to total phenolic compound identification in actual fruit samples (strawberry, blueberry, apple, pear, and grapes) with a diverse number of phenolic compounds, comparing the outcomes with the classical spectrophotometric technique as standard values.

Using integrated MOF with Au microelectrode (μE), a new electrochemical micro analytical device (EμAD) was developed for chlorpyrifos determination.[59] MOF are used as a matrix unit to construct EμAD incorporated with the AChE enzyme to enable the sensitivity and specificity of the sensor. The applicability of the EμAD probe for chlorpyrifos sensing in actual vegetable samples has also been explored (Fig. 6). The current study incorporates the EμAD with a portable potentiostat (k-Stat) with a bluetooth interface, which enables overall device miniaturization for real-time OP determination. More recently, Rashid's group introduced an effective approach for the fabrication of an S-scheme flower-like NiSe-Fe_3O_4/C heterostructure stemmed from MIL-88(Ni/Fe) and employed toward TC photo-degradation in an as-prepared spiral form microfluidic photoreactor.[85] Design of the Fe_3O_4 (as a p-type semiconductor), and NiSe heterostructure (as an n-type semiconductor), not only show brilliant activity owing to their photoexcited charge transfer and good conductivity but also owing to their magnetic capability to enhance the regeneration and separation of photocatalyst with the help of external magnetic field after the treatment procedure.[86] In addition, the combination of different characterization methods, design of experiment models, and density functional theory calculations, with the help of microfluidic chips are applied for assessing the building performance relationships. Meng and coworkers employed a biological barcode NM using a MOF to enhance the response of an aptamer toward streptomycin finding great diagnostic recognizability (LOD of 4.5 pM). The detecting interface was basically constructed by anchoring a mixed mono-sheet of 6-mercapto-1-hexanol (MCH) and thiolated cDNA/aptamer duplexes on the AuNPs modified screen printed carbon electrodes (SPCE). Then, a MOF-derived biological barcode is integrated into the modified surface. Metal-organic framework is a new material that gives high surface area with great pore volume and in this study was modified with AuNPs to attach the bar codes (DNA strands). Therefore, a high volume of DNA strands could be immobilized causing a greater redox probe adsorption (applied for indirect detection of streptomycin). This nanoprobe is selective to other antibiotics like OTC, kanamycin, and CAP, and can be used for the exploration of spiked milk samples, that have membrane filtration, and centrifugation. No data on the nanoprobe stability was given.[60]

Wang et al[61] introduced a dual catalytic enhancement

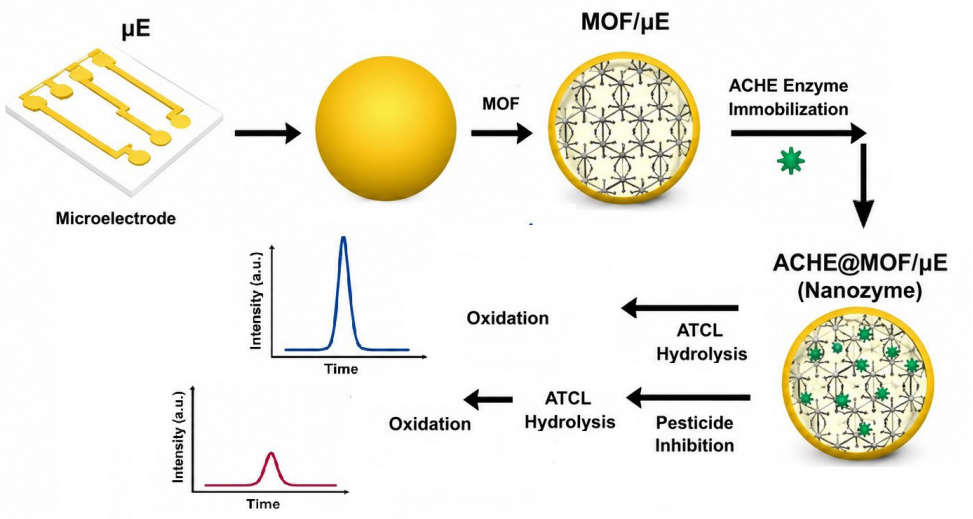

Fig. 6. Schematic of the step-wise electrode (EμAD) construction toward chlorpyrifos sensing. The system comprises the Au microelectrode with the all-in-one electrochemical analyzer and microfluidic substrate for the identification of electroactive species. Reprinted with permission from Nagabooshanam et al[59] under the Creative Commons Attribution 4.0 International License (https://creativecommons.org/licenses/by/4.0/).

approach utilizing Fe_3O_4 nanozyme-supported carbon QDs (C-dots)@Ag-MOFs as current amplification components. According to this approach, a new electrochemical microfluidic paper-based chip was developed for the detection of parathion-methyl, a significant insecticide. Fe_3O_4/C-dots@Ag-MOFs were produced through a hydrothermal process, followed by the synthesis of a MIP on the modified surface using parathion-methyl as a template molecule. Subsequently, the reaction area of a chip was tailored with MIP/Fe_3O_4/C-dots@Ag-MOFs. Parathion-methyl present in the sample presented into the response region was captured by the MIP, resulting in a decreased current response at -0.53 V (vs. Ag/AgCl reference electrode) in a three-electrode system integrated within the chip. Simultaneous catalysis via Ag-MOFs and Fe_3O_4/C-dots considerably boosted the signal. The microchip demonstrated a LOD of 11.6 pM and was effectively utilized for quantifying parathion-methyl in environmental samples and agricultural products with recovery rates of 82.7%-109%. By integrating a dual catalytic amplification approach with the MIP method, this platform substantially enhanced the sensitivity and specificity of the microfluidic paper-based chips.

Covalent organic frameworks have garnered significant interest because of their advantageous characteristics, such as structure adjustability, good aperture, abundant functional groups, and exceptional adsorption capabilities, which make COFs highly promising for applications in sensing, storage, catalysis, sample preparation, and other related fields.[83] For instance, a rational design of COF activated with artificial anodic aluminum oxide (AAO) as a microfluidic system was reported for the precise and rapid quantification of Hg.[62] As a proof of concept, a COF linked with thiourea (JNU-3) as the recognition element is covalently attached to the stable AAO nanochannels in order to create a microfluidic sensor based on JNU-3@AAO. The high specific affinity of thiourea-connected JNU-3 to Hg(II) and its well-structured channels would enhance the kinetics and selectivity of JNU-3@AAO for detecting Hg(II) with a broad concentration range (0.01-100 pg mL^{-1}), low LOD (3.28 fg mL^{-1}), and good precision. The established technique was effectively utilized to analyze the levels of Hg in certified reference material A072301c (rice powder), rice samples, and real water, yielding recoveries ranging from 90.4% to 99.8%. This study demonstrates the significant promise of utilizing COFs-modified solid-state microfluidic channels as a sensor for the accurate and rapid identification of pollutants in complex samples.

Numerous existing systems continue to depend on complex synthesis methodologies, exhibit limited material stability under harsh environmental conditions, and demonstrate relatively poor long-term reproducibility. Furthermore, the incorporation of MOFs and COFs into flexible and scalable microfluidic platforms remains a significant technical challenge, primarily due to issues related to material immobilization and the preservation of structural integrity during continuous fluid flow. Consequently, future research should prioritize the development of environmentally stable and cost-effective framework materials, the enhancement of integration techniques for portable and wearable sensing devices, and the investigation of multifunctional hybrid structures that synergistically combine MOFs or COFs with conductive NMs, enzymes, aptamers, or molecularly imprinted polymers.

Intelligent microfluidics

AI encapsulates the emulation of human cognitive functions by machines, chiefly computational systems. These cognitive functions encompass learning, logical deduction, and adaptive modification.[87] The utilization of AI technologies is progressively prevalent across numerous domains, aimed at streamlining operations, augmenting efficiency, and refining decision-making frameworks.[88] The incorporation of machine learning with microfluidics is emerging in novel and innovative forms, leading to the development of new scientific research that is increasingly being referred to in the literature as "intelligent microfluidics", which is depicted in Fig. 7.[89-91]

Microfluidics inherently produces large volumes of data by efficiently performing automated tasks at the micrometer scale. However, effective control and information extraction from these processes necessitate the automatic retrieval and processing of the data generated by the platform.[92] A frequently cited example

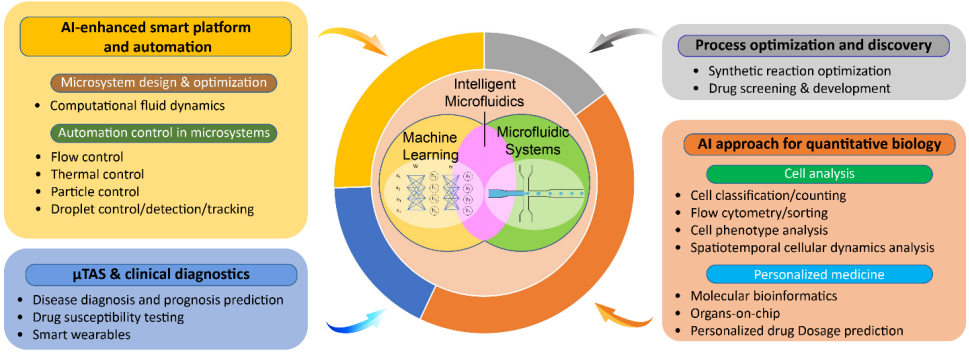

Fig. 7. Diagram of microfluidic applications integrated with AI. Reprinted from Tsai et al[89] under the Creative Commons Attribution 4.0 International License (https://creativecommons.org/licenses/by/4.0/).

that leverages this interaction is microdroplet generation, a highly studied high-throughput process to which microfluidics has significantly contributed. In this notably fascinating context, machine learning algorithms served as tools to enhance the optimization of microdroplet generation and their identification through "barcodes." These barcodes, which may consist of substances such as DNA or dyes, or specific droplet sequences, enable the differentiation of the contents of one droplet from another.[93,94] Concurrently, machine learning has been shown to represent a novel and compelling approach for optimizing microfluidic platforms, including the refinement of device geometries and the modulation of fluid flow within these systems.[95] An additional noteworthy contribution in this domain was presented by Rizkin et al, who developed an advanced microreactor system to investigate polymerization reactions utilizing infrared thermography combined with deep learning techniques.[96]

Furthermore, when investigating flow distribution within a microfluidic chip from a theoretical or simulation-based perspective, the Navier-Stokes equations are widely recognized as providing an accurate representation of the dynamics of viscous fluids. Nonetheless, the existence of general solutions to these equations remains unresolved, constituting one of the seven Millennium Prize Problems identified by the Clay Mathematics Institute.[97] Furthermore, non-ideal factors affecting microfluidic devices, such as surface roughness, intricate geometrical configurations, and multiphysics interactions, can progressively complicate the determination of the flow distribution.[98] Machine learning is increasingly demonstrating its potential in this domain by approximating flow dynamics in real-time scenarios, rapidly changing, where traditional finite element method (FEM) simulations are prohibitively time-consuming.[99] For instance, a deep learning methodology has been developed to simulate particle manipulation by employing a neural network capable of capturing the underlying flow physics from particle motion and fluidic control inputs.[100] Subsequently, the system was incorporated into a reinforcement learning-based controller, an approach that will be examined in greater detail in the following sections, to enable a smart fluidic micromanipulator.

The IoT comprises a constellation of interlinked devices capable of communicating and exchanging information amongst one another. These devices encompass a spectrum from commonplace household items to intricate industrial apparatus.[101] Internet of things technology facilitates the aggregation and examination of substantial data volumes, thereby enabling enhanced surveillance, regulation, and optimization of varied systems.[102] The amalgamation of AI and IoT harbors the potential to transform our engagement with technology and the surrounding environment. By synthesizing AI's proficiency in data analysis and interpretation with IoT's connectivity and data integration capabilities, we can engineer more astute and efficient systems. One domain where this convergence exhibits considerable potential is in microfluidic sensors leveraging NMs. The integration of AI and IoT technologies within microfluidic sensors, particularly those employing NMs, can yield the development of exceptionally sensitive and specific detection systems for an array of food and environmental samples.[103] AI algorithms can process data acquired from these sensors instantaneously, delivering valuable insights and expediting decision-making processes. Concurrently, IoT connectivity facilitates remote oversight and administration of these sensors, augmenting their adaptability and accessibility across diverse applications.[104]

Notwithstanding the encouraging prospects associated with NM-based microfluidic sensors, there exists a significant deficiency in their amalgamation with IoT and AI technologies for the purpose of detecting analytes within food and environmental matrices. This shortfall is attributable to various challenges, encompassing the complex fabrication methodologies of NMs, the imperative for sophisticated signal processing to decode intricate data, as well as the requirement for real-time monitoring functionalities that IoT solutions are capable of offering. To rectify this predicament, interdisciplinary collaboration among materials scientists, engineers, and data analysts is crucial in order to optimize sensor design and advance data analysis methodologies. Furthermore, allocating resources towards the development of user-centric platforms that integrate these technologies may promote wider adoption and progressive development, ultimately culminating in the establishment of more resilient monitoring systems for food safety and environmental stewardship.

Conclusion and future prospective

The widespread and improper use of chemical contaminants, including antibiotics, pesticides, and heavy metals, constitutes a significant global concern. This issue poses a serious threat to both the ecological environment and human health. Accurate and rapid quantification of these pollutants is crucial for ensuring food safety and reducing the incidence of foodborne diseases. Microfluidics has emerged as a powerful tool for the analysis of chemical contaminants, particularly within the context of POCT. The incorporation of NMs into microfluidic technology holds significant promise for enhancing the analytical capabilities of microfluidic systems in detecting chemical contaminants across various applications; i) Target isolation can be accurately regulated by manipulating the magnetic properties of magnetic NMs; ii) Enhanced target separation efficiency is attained by increasing the binding surface area of chips through the inherently straightforward functionalization process and a higher surface-area-to-volume ratio. This can be exemplified by the use of NPs and nanorods; and iii) The signal readout is enhanced in terms of multiplexity and sensitivity by leveraging the unique characteristics of

QDs and metal NMs, including their catalytic activity, optical properties, and electrical conductivity. Despite significant advancements, challenges remain, and certain areas require further investigation. Moreover, the practical application of NM-based microfluidic systems remains to encounter challenges, while they reveal outstanding analytical performance in laboratory settings. The construction of microfluidic devices commonly necessitates costly and complex processes, which may hinder commercialization and large-scale manufacturing. Additionally, the reliability between produced devices and the long-term stability of nanomaterials within intricate environmental and food matrices are substantial issues. A comparative analysis of sensing mechanisms, such as colorimetric, SERS, electrochemical, and fluorescence methods, exposes that each approach has unique profits and disadvantages based on analytical circumstances and the target contaminant. Also, validation with real-world samples, the standardization of fabrication methods, and cost-effectiveness must be carefully considered in advance of reaching extensive point-of-care and industrial implementation. (1) The consistent production of NP batches remains a significant challenge. The functionality of NPs is profoundly influenced by their quality, including parameters such as shape, size, and uniformity. Therefore, there is an urgent need to develop reliable methodologies for synthesizing NPs that demonstrate consistent quality, stability, and sufficient performance for analytical applications. (2) The primary challenges in ground sensing are the reproducibility and accuracy of results, which stem from the absence of established standards and normalization protocols for NM-centered microfluidic systems. Each NM demonstrates efficacy within specific parameters, highlighting the need for standardizing nanotechnologies to ensure consistent and reliable outcomes. (3) To improve the detection and separation capabilities of a single NM-based microfluidic chip, it is crucial to carefully select recognition units such as aptamers, antibodies, peptides, and nucleic acids. This selection enables controlled release and specific capture of target analytes. Additionally, it is essential to thoroughly evaluate the potential biological toxicity of NPs. (4) The simultaneous detection of multiple antibiotics and pesticides is essential due to their potential coexistence in contaminated food sources. A promising approach involves using multiple nanoprobes or employing various segmented regions. Therefore, it is crucial to integrate NPs with distinct properties—such as plasmonic, magnetic, or fluorescent characteristics—into a single nanostructured entity or to develop novel luminescent NPs that exhibit precise, narrow emission spectra. This strategy can help reduce spectral cross-talk among different diagnostic channels. (5) The need for specialized devices to interpret signals associated with point-of-care testing (POCT) poses a significant barrier to its widespread adoption, primarily due to the complexities involved in their development. However, there is increasing emphasis on advancements in this area, as demonstrated by the growing use of handheld and simplified tools. Instruments used to ensure food safety include pH meters, glucose meters, digital multimeters, pressure meters, thermometers, and AI technologies, particularly those integrated into mobile devices, which enable straightforward operation. The signals generated can be monitored in real time via smartphone applications equipped with self-programming software, allowing wireless transmission of results to other users.

In conclusion, the field of NM-based microfluidics is expected to advance alongside developments in NM engineering, including functionalization and synthesis, as well as improvements in chip design, such as cost-effectiveness, portability, automation, and real-time separation and identification. Moreover, integrating AI and the IoT into microfluidic sensors will be crucial for enhancing data analytics, enabling instantaneous monitoring, and facilitating more effective decision-making across various applications. Additionally, the broad applicability of these technologies, exemplified by dual-mode signal readout and multiplexed analysis, is likely to increase their utility.

Acknowledgements

Authors gratefully acknowledge the Research Center for Pharmaceutical Nanotechnology, Tabriz University of Medical Sciences for the supporting of this work.

Authors' Contribution

Conceptualization: Zahra Karimzadeh.
Data curation: Mansour Mahmoudpour.
Formal analysis: Saeid Karimzadeh, Mansour Mahmoudpour.
Funding acquisition: Zahra Karimzadeh.
Investigation: Saeid Karimzadeh, Mir-Michael Mousavi.
Methodology: Mansour Mahmoudpour, Zahra Karimzadeh.
Project administration: Zahra Karimzadeh.
Resources: Zahra Karimzadeh.
Supervision: Zahra Karimzadeh.
Validation: Zahra Karimzadeh, Mansour Mahmoudpour.
Visualization: Mansour Mahmoudpour.
Writing—original draft: Saeid Karimzadeh, Mir-Michael Mousavi.
Writing—review & editing: Mansour Mahmoudpour, Zahra Karimzadeh.

Competing Interests

The authors declare that they have no known competing financial interests or personal relationships that could have appeared to influence the work reported in this paper.

Data Availability Statement

Data sharing not applicable to this article.

Declaration of AI-assisted Tools in the Writing Procedure

We utilized AI tool (ChatGPT) to assist in correcting the English writing and enhancing the readability and language of the manuscript, which was subsequently reviewed and controlled by the authors. We confirm that AI-assisted tools were not used in the creation of any figures or graphical abstracts included in this manuscript.

Ethical Approval

Not applicable.

Funding

This work is financially supported by the Research Center for Pharmaceutical Nanotechnology, Tabriz University of Medical Sciences, Tabriz, Iran, under grant number 78886.

References

1. Bilal M, Shabbir MA, Iqbal W, Ullah S, Asim M, Arslan M, et al. Innovative advances in colorimetric sensor array technology for food safety and quality assessment: an updated comprehensive review. *Food Rev Int* **2026**; 42: 1797-822. doi:10.1080/87559129.2025.2526677
2. Hong E, Lee SY, Jeong JY, Park JM, Kim BH, Kwon K, et al. Modern analytical methods for the detection of food fraud and adulteration by food category. *J Sci Food Agric* **2017**; 97: 3877-96. doi:10.1002/jsfa.8364
3. Karimzadeh Z, Mahmoudpour M, de la Guardia M, Ezzati Nazhad Dolatabadi J, Jouyban A. Aptamer-functionalized metal organic frameworks as an emerging nanoprobe in the food safety field: promising development opportunities and translational challenges. *Trends Analyt Chem* **2022**; 152: 116622. doi:10.1016/j.trac.2022.116622
4. Garg M, Pamme N. Microfluidic (bio)-sensors based on 2-D layered materials. *Trends Analyt Chem* **2023**; 158: 116839. doi:10.1016/j.trac.2022.116839
5. Nix C, Ghassemi M, Crommen J, Fillet M. Overview on microfluidics devices for monitoring brain disorder biomarkers. *Trends Analyt Chem* **2022**; 155: 116693. doi:10.1016/j.trac.2022.116693
6. Chen S, Sun Y, Fan F, Chen S, Zhang Y, Zhang Y, et al. Present status of microfluidic PCR chip in nucleic acid detection and future perspective. *Trends Analyt Chem* **2022**; 157: 116737. doi:10.1016/j.trac.2022.116737
7. Berlanda SF, Breitfeld M, Dietsche CL, Dittrich PS. Recent advances in microfluidic technology for bioanalysis and diagnostics. *Anal Chem* **2021**; 93: 311-31. doi:10.1021/acs.analchem.0c04366
8. Amreen K, Ramya K, Goel S. Microfluidic devices for synthesizing nanomaterials. In: *Microfluidics in Food Processing*. CRC Press; **2025**. p. 106-27.
9. Qu X, Ma J, Zeng D, Luo J, Wu J, Liu C, et al. Microcavity-assisted microfluidic physical sensors: materials, structures, and multifunctional applications. *Lab Chip* **2026**; 26: 1394-416. doi:10.1039/d5lc00822k
10. Preetam S, Mishra R, Alghamdi S, Aslam A, Thapliyal S, Rustagi S, et al. Recent advances in microfluidic technologies for the detection of Alzheimer's disease biomarkers: toward point-of-care neurodiagnostic. *Mikrochim Acta* **2026**; 193: 203. doi:10.1007/s00604-026-07962-3
11. Ao F, An Y, Jia W. Interface control in detectors: Enhancing the sensitivity of paper-based microfluidic chips for biomarker detection. *Colloids Surf B Biointerfaces* **2026**; 266: 115766. doi:10.1016/j.colsurfb.2026.115766
12. Zhang J, Misra RDK. Nanomaterials in microfluidics for disease diagnosis and therapy development. *Mater Technol* **2019**; 34: 92-116. doi:10.1080/10667857.2018.1527803
13. Wang Y, Gao Y, Yin Y, Pan Y, Wang Y, Song Y. Nanomaterial-assisted microfluidics for multiplex assays. *Microchim Acta* **2022**; 189: 139. doi:10.1007/s00604-022-05226-4
14. Fattahi Z, Hasanzadeh M. Nanotechnology-assisted microfluidic systems for chemical sensing, biosensing, and bioanalysis. *Trends Analyt Chem* **2022**; 152: 116637. doi:10.1016/j.trac.2022.116637
15. Chen T, Yin S, Wu J. Nanomaterials meet microfluidics: improved analytical methods and high-throughput synthetic approaches. *Trends Analyt Chem* **2021**; 142: 116309. doi:10.1016/j.trac.2021.116309
16. Shang Y, Xiang X, Ye Q, Wu Q, Zhang J, Lin J-M. Advances in nanomaterial-based microfluidic platforms for on-site detection of foodborne bacteria. *Trends Analyt Chem* **2022**; 147: 116509. doi:10.1016/j.trac.2021.116509
17. Yang Z, Xu T, Li H, She M, Chen J, Wang Z, et al. Zero-dimensional carbon nanomaterials for fluorescent sensing and imaging. *Chem Rev* **2023**; 123: 11047-136. doi:10.1021/acs.chemrev.3c00186
18. Fang H, Zhu D, Yang Q, Chen Y, Zhang C, Gao J, et al. Emerging zero-dimensional to four-dimensional biomaterials for bone regeneration. *J Nanobiotechnology* **2022**; 20: 26. doi:10.1186/s12951-021-01228-1
19. Gong S, Cheng W. One-dimensional nanomaterials for soft electronics. *Adv Electron Mater* **2017**; 3: 1600314. doi:10.1002/aelm.201600314
20. Shin J, Kang N, Kim B, Hong H, Yu L, Kim J, et al. One-dimensional nanomaterials for cancer therapy and diagnosis. *Chem Soc Rev* **2023**; 52: 4488-514. doi:10.1039/d2cs00840h
21. Rao CN, Sood AK, Subrahmanyam KS, Govindaraj A. Graphene: the new two-dimensional nanomaterial. *Angew Chem Int Ed Engl* **2009**; 48: 7752-77. doi:10.1002/anie.200901678
22. Tan C, Cao X, Wu XJ, He Q, Yang J, Zhang X, et al. Recent advances in ultrathin two-dimensional nanomaterials. *Chem Rev* **2017**; 117: 6225-331. doi:10.1021/acs.chemrev.6b00558
23. Baghal Behyar M, Hasanzadeh M, Seidi F, Shadjou N. Sensing of amino acids: critical role of nanomaterials for the efficient biomedical analysis. *Microchem J* **2023**; 188: 108452. doi:10.1016/j.microc.2023.108452
24. Shehzad K, Xu Y, Gao C, Duan X. Three-dimensional macro-structures of two-dimensional nanomaterials. *Chem Soc Rev* **2016**; 45: 5541-88. doi:10.1039/c6cs00218h
25. O'Brien CM, Holmes B, Faucett S, Zhang LG. Three-dimensional printing of nanomaterial scaffolds for complex tissue regeneration. *Tissue Eng Part B Rev* **2015**; 21: 103-14. doi:10.1089/ten.TEB.2014.0168
26. Baghal Behyar M, Mirzaie A, Hasanzadeh M, Shadjou N. Advancements in biosensing of hormones: recent progress and future trends. *Trends Analyt Chem* **2024**; 173: 117600. doi:10.1016/j.trac.2024.117600
27. Tavakoli H, Mohammadi S, Li X, Fu G, Li X. Microfluidic platforms integrated with nano-sensors for point-of-care bioanalysis. *Trends Analyt Chem* **2022**; 157: 116806. doi:10.1016/j.trac.2022.116806
28. Rasheed S, Ul Haq MA, Ahmad N, Sirajuddin, Hussain D. Smartphone-integrated colorimetric and microfluidic paper-based analytical devices for the trace-level detection of permethrin. *Food Chem* **2023**; 429: 136925. doi:10.1016/j.foodchem.2023.136925
29. Taheri H, Khayatian G. Smartphone-based microfluidic chip modified using pyrrolidine-1-dithiocarboxylic acid for simultaneous colorimetric determination of Cr3 + and Al3 + ions. *Spectrochim Acta A Mol Biomol Spectrosc* **2022**; 272: 121000. doi:10.1016/j.saa.2022.121000
30. Zhang K, Gan N, Shen Z, Cao J, Hu F, Li T. Microchip electrophoresis based aptasensor for multiplexed detection of antibiotics in foods via a stir-bar assisted multi-arm junctions recycling for signal amplification. *Biosens Bioelectron* **2019**; 130: 139-46. doi:10.1016/j.bios.2019.01.044
31. Zeng L, Liu L, Kuang H, Cui G, Xu C. A paper-based colorimetric assay for rapid detection of four macrolides in milk. *Mater Chem Front* **2019**; 3: 2175-83. doi:10.1039/c9qm00429g
32. Wang Y, Rink S, Baeumner AJ, Seidel M. Microfluidic flow-injection aptamer-based chemiluminescence platform for sulfadimethoxine detection. *Mikrochim Acta* **2022**; 189: 117. doi:10.1007/s00604-022-05216-6
33. Chattopadhyay S, Sabharwal PK, Jain S, Kaur A, Singh H. Functionalized polymeric magnetic nanoparticle assisted SERS immunosensor for the sensitive detection of *S. typhimurium*. *Anal Chim Acta* **2019**; 1067: 98-106. doi:10.1016/j.aca.2019.03.050
34. Wu H, Luo Y, Hou C, Huo D, Zhou Y, Zou S, et al. Flexible bipyramid-AuNPs based SERS tape sensing strategy for detecting methyl parathion on vegetable and fruit surface. *Sens Actuators B Chem* **2019**; 285: 123-8. doi:10.1016/j.snb.2019.01.038
35. Yan S, Chu F, Zhang H, Yuan Y, Huang Y, Liu A, et al. Rapid, one-step preparation of SERS substrate in microfluidic channel for detection of molecules and heavy metal ions. *Spectrochim Acta A Mol Biomol Spectrosc* **2019**; 220: 117113. doi:10.1016/j.saa.2019.05.018
36. Zhang H, Wang D, Zhang D, Zhang T, Yang L, Li Z. In situ microfluidic SERS chip for ultrasensitive Hg2 + sensing based on I(-)-functionalized silver aggregates. *ACS Appl Mater Interfaces* **2022**; 14: 2211-8. doi:10.1021/acsami.1c17832
37. Chen X, Wang J, Shen HY, Su X, Cao Y, Li T, et al. Microfluidic chip for multiplex detection of trace chemical contaminants based on magnetic encoded aptamer probes and multibranched DNA nanostructures as signal tags. *ACS Sens* **2019**; 4: 2131-9. doi:10.1021/acssensors.9b00963
38. Mei Y, Yang S, Li C, Li X, Yu Y, Liu R, et al. A novel visual biosensor for mercury detection based on a cleavable phosphorothioate-RNA probe and microfluidic bead trap. *Microchem J* **2023**; 195:

109462. doi:10.1016/j.microc.2023.109462
39. Écija-Arenas Á, Román-Pizarro V, Fernández-Romero JM. Usefulness of hybrid magnetoliposomes for aminoglycoside antibiotic residues determination in food using an integrated microfluidic system with fluorometric detection. *J Agric Food Chem* **2021**; 69: 6888-96. doi:10.1021/acs.jafc.1c01571
40. Zhang Z, Ma X, Jia M, Li B, Rong J, Yang X. Deposition of CdTe quantum dots on microfluidic paper chips for rapid fluorescence detection of pesticide 2,4-D. *Analyst* **2019**; 144: 1282-91. doi:10.1039/c8an02051e
41. Zhou J, Li B, Qi A, Shi Y, Qi J, Xu H, et al. ZnSe quantum dot-based ion imprinting technology for fluorescence detecting cadmium and lead ions on a three-dimensional rotary paper-based microfluidic chip. *Sens Actuators B Chem* **2020**; 305: 127462. doi:10.1016/j.snb.2019.127462
42. Abdollahian P, Heidari H, Hassanzadeh S, Hasanzadeh M. Accelerated naked-eye identification of cations using non-plasmonic amplification by functionalized GQDs: a novel photochemical microfluidic sensor for environmental/mineral analysis using Lab-on-paper technology. *J Photochem Photobiol A Chem* **2024**; 448: 115299. doi:10.1016/j.jphotochem.2023.115299
43. Li T, Guo G, Xing H, Tang S, Hu H, Wang L, et al. Construction of fluorescent sensor array and three-dimensional microfluidic paper based analytical device for specific identification and visual determination of antibiotics in food. *Food Chem* **2023**; 429: 136947. doi:10.1016/j.foodchem.2023.136947
44. Yang Y, Tong X, Chen Y, Zhou R, Cai G, Wang T, et al. A dual-emission carbon dots-based nonenzymatic fluorescent sensing platform for simultaneous detection of parathion-methyl and glyphosate. *Food Chem* **2023**; 403: 134346. doi:10.1016/j.foodchem.2022.134346
45. Tong X, Cai G, Xie L, Wang T, Zhu Y, Peng Y, et al. Threaded 3D microfluidic paper analytical device-based ratiometric fluorescent sensor for background-free and visual detection of organophosphorus pesticides. *Biosens Bioelectron* **2023**; 222: 114981. doi:10.1016/j.bios.2022.114981
46. Li G, Liu C, Zhang X, Zhai P, Lai X, Jiang W. Low temperature synthesis of carbon dots in microfluidic chip and their application for sensing cefquinome residues in milk. *Biosens Bioelectron* **2023**; 228: 115187. doi:10.1016/j.bios.2023.115187
47. Li T, Guo G, Xing H, Wang Y, Luo X, Wang L, et al. Energy transfer mediated rapid and visual discrimination of tetracyclines and quercetin in food by using N, Cu co-doped carbon dots. *Anal Chim Acta* **2023**; 1239: 340706. doi:10.1016/j.aca.2022.340706
48. Tong X, Lin X, Duan N, Wang Z, Wu S. Laser-printed paper-based microfluidic chip based on a multicolor fluorescence carbon dot biosensor for visual determination of multiantibiotics in aquatic products. *ACS Sens* **2022**; 7: 3947-55. doi:10.1021/acssensors.2c02008
49. Cheng Y, Chen Z, Wang Y, Xu J. Continuous synthesis of N, S co-coped carbon dots for selective detection of CD(II) ions. *J Photochem Photobiol A Chem* **2022**; 429: 113910. doi:10.1016/j.jphotochem.2022.113910
50. Al-Jaf SH, Omer KM. Dual-spot ratiometric microfluidic paper-based analytical device for accuracy and precision improvement. *Talanta* **2024**; 269: 125433. doi:10.1016/j.talanta.2023.125433
51. Islam S, Shukla S, Bajpai VK, Han YK, Huh YS, Ghosh A, et al. Microfluidic-based graphene field effect transistor for femtomolar detection of chlorpyrifos. *Sci Rep* **2019**; 9: 276. doi:10.1038/s41598-018-36746-w
52. Chungchai W, Amatatongchai M, Meelapsom R, Seebunrueng K, Suparsorn S, Jarujamrus P. Development of a novel three-dimensional microfluidic paper-based analytical device (3D-μPAD) for chlorpyrifos detection using graphene quantum-dot capped gold nanocomposite for colorimetric assay. *Int J Environ Anal Chem* **2020**; 100: 1160-78. doi:10.1080/03067319.2019.1650921
53. Kunpatee K, Kalcher K, Chailapakul O, Chaiyo S, Samphao A. A paper chromatographic-based electrochemical analytical device for the separation and simultaneous detection of carbofuran and carbaryl pesticides. *Sens Actuators B Chem* **2023**; 377: 133116. doi:10.1016/j.snb.2022.133116
54. Park M, Seo TS. An integrated microfluidic device with solid-phase extraction and graphene oxide quantum dot array for highly sensitive and multiplex detection of trace metal ions. *Biosens Bioelectron* **2019**; 126: 405-11. doi:10.1016/j.bios.2018.11.010
55. Ma S, Zhao W, Zhang Q, Zhang K, Liang C, Wang D, et al. A portable microfluidic electrochemical sensing platform for rapid detection of hazardous metal Pb2+based on thermocapillary convection using 3D Ag-rGO-f-NiOH2/NF as a signal amplifying element. *J Hazard Mater* **2023**; 448: 130923. doi:10.1016/j.jhazmat.2023.130923
56. Zhang J, Shi G. Rational design of MoS2 QDs and Eu3+as a ratiometric fluorescent probe for point-of-care visual quantitative detection of tetracycline via smartphone-based portable platform. *Anal Chim Acta* **2022**; 1198: 339572. doi:10.1016/j.aca.2022.339572
57. Zhang Y, Zhou S, Liu H, Tang X, Zhou H, Cai H. Nitrogen-doped MoS2 QDs as fluorescent probes for sequential dual-target detection and their microfluidic logic gate operations. *Microchem J* **2021**; 169: 106553. doi:10.1016/j.microc.2021.106553
58. Martínez-Pérez-Cejuela H, Mesquita RB, Simó-Alfonso EF, Herrero-Martínez JM, Rangel A. Combining microfluidic paper-based platform and metal-organic frameworks in a single device for phenolic content assessment in fruits. *Mikrochim Acta* **2023**; 190: 126. doi:10.1007/s00604-023-05702-5
59. Nagabooshanam S, Roy S, Mathur A, Mukherjee I, Krishnamurthy S, Bharadwaj LM. Electrochemical micro analytical device interfaced with portable potentiostat for rapid detection of chlorpyrifos using acetylcholinesterase conjugated metal organic framework using internet of things. *Sci Rep* **2019**; 9: 19862. doi:10.1038/s41598-019-56510-y
60. Meng X, Gu H, Yi H, He Y, Chen Y, Sun W. Sensitive detection of streptomycin in milk using a hybrid signal enhancement strategy of MOF-based bio-bar code and target recycling. *Anal Chim Acta* **2020**; 1125: 1-7. doi:10.1016/j.aca.2020.05.041
61. Li S, Pang C, Ma X, Zhang Y, Xu Z, Li J, et al. Microfluidic paper-based chip for parathion-methyl detection based on a double catalytic amplification strategy. *Mikrochim Acta* **2021**; 188: 438. doi:10.1007/s00604-021-05084-6
62. Ran XQ, Qian HL, Yan XP. Integrating ordered two-dimensional covalent organic frameworks to solid-state nanofluidic channels for ultrafast and sensitive detection of mercury. *Anal Chem* **2022**; 94: 8533-8. doi:10.1021/acs.analchem.2c01595
63. Li J, Ma J, Sun H, Yu M, Wang H, Meng Q, et al. Transformation of arginine into zero-dimensional nanomaterial endows the material with antibacterial and osteoinductive activity. *Sci Adv* **2023**; 9: eadf8645. doi:10.1126/sciadv.adf8645
64. Pedireddy S, Lee HK, Tjiu WW, Phang IY, Tan HR, Chua SQ, et al. One-step synthesis of zero-dimensional hollow nanoporous gold nanoparticles with enhanced methanol electrooxidation performance. *Nat Commun* **2014**; 5: 4947. doi:10.1038/ncomms5947
65. Venugopalan P, Samad SA, Kumawat N, Kumar S. Plasmonic sensing in microfluidic paper-based analytical devices integrated with metal nanoparticles: a review. *RSC Adv* **2025**; 15: 31723-51. doi:10.1039/d5ra01972a
66. Shrivastav AM, Cvelbar U, Abdulhalim I. A comprehensive review on plasmonic-based biosensors used in viral diagnostics. *Commun Biol* **2021**; 4: 70. doi:10.1038/s42003-020-01615-8
67. Adeeyo AO, Alabi MA, Oyetade JA, Nkambule TT, Mamba BB, Oladipo AO, et al. Magnetic nanoparticles: advances in synthesis, sensing, and theragnostic applications. *Magnetochemistry* **2025**; 11: 9. doi:10.3390/magnetochemistry11020009
68. Akbarzadeh A, Samiei M, Davaran S. Magnetic nanoparticles: preparation, physical properties, and applications in biomedicine. *Nanoscale Res Lett* **2012**; 7: 144. doi:10.1186/1556-276x-7-144
69. Wang W, Zhou R, Jayan H, Yin L, Shao X, Zou X, et al. Innovative applications of quantum dots-based surface-enhanced Raman spectroscopy for food safety detection. *Crit Rev Food Sci Nutr* **2026**; 66: 791-810. doi:10.1080/10408398.2025.2531224
70. Du F, Chen R, Feng E, Dai H, Yu F. Near-infrared I/II fluorescent carbon dots: tailoring synthesis and optical properties for biomedical applications. *Coord Chem Rev* **2026**; 551: 217460. doi:10.1016/j.ccr.2025.217460
71. Kayani KF. Red emissive carbon dots (R-CDs) and their analytical sensing applications. *Microchem J* **2026**; 225: 118088. doi:10.1016/j.

microc.2026.118088
72. Han J, Liu F, Qi J, Arabi M, Li W, Wang G, et al. A ZnFe2O4-catalyzed segment imprinted polymer on a three-dimensional origami paper-based microfluidic chip for the detection of microcystin. *Analyst* **2022**; 147: 1060-5. doi:10.1039/d2an00032f
73. Moulahoum H, Ghorbanizamani F, Guler Celik E, Timur S. Nano-scaled materials and polymer integration in biosensing tools. *Biosensors (Basel)* **2022**; 12: 301. doi:10.3390/bios12050301
74. Feng S, Lin Y, Xu J, Lu X. Inertial microfluidic-assisted rapid detection of chemical contaminant in foods using quantum dots-based molecularly imprinted sensor. *Sens Actuators B Chem* **2023**; 394: 134342. doi:10.1016/j.snb.2023.134342
75. Sheeraz AS, Kumara BN, Pereira P, Dsilva DJ, Mohanty PS, Prasad KS. Miniaturized 3D printed microfluidic polymeric-paper hybrid device for colorimetric detection of arsenic (III). *ChemistrySelect* **2025**; 10: e00277. doi:10.1002/slct.202500277
76. Hu T, Mei X, Wang Y, Weng X, Liang R, Wei M. Two-dimensional nanomaterials: fascinating materials in biomedical field. *Sci Bull (Beijing)* **2019**; 64: 1707-27. doi:10.1016/j.scib.2019.09.021
77. Pethe A, Priyadarshini S, Chamoli S, Tripathi D, Karki K, Khondekar KR, et al. Graphene oxide-based DNA biosensing: recent advances and emerging roles of artificial intelligence and machine learning. *Microchem J* **2026**; 222: 117219. doi:10.1016/j.microc.2026.117219
78. Surya Bhaskaram D. Raman spectroscopy of reduced graphene oxide: a review highlighting defect-induced bands and a glimpse into machine learning approaches. *Crit Rev Anal Chem* **2026**: 1-16. doi:10.1080/10408347.2026.2615687
79. Chan C, Shi J, Fan Y, Yang M. A microfluidic flow-through chip integrated with reduced graphene oxide transistor for influenza virus gene detection. *Sens Actuators B Chem* **2017**; 251: 927-33. doi:10.1016/j.snb.2017.05.147
80. Di Santo R, Digiacomo L, Palchetti S, Palmieri V, Perini G, Pozzi D, et al. Microfluidic manufacturing of surface-functionalized graphene oxide nanoflakes for gene delivery. *Nanoscale* **2019**; 11: 2733-41. doi:10.1039/c8nr09245a
81. Sharma BB. From the rise of 2D nanomaterials to high-performance separation membranes: a critical review. *ACS Appl Eng Mater* **2026**; 4: 429-47. doi:10.1021/acsaenm.5c00974
82. Chen H, Luo B, Wu S, Shi S, Dai Q, Peng Z, et al. Microfluidic biosensor based on molybdenum disulfide (MoS2) modified thin-core microfiber for immune detection of *Toxoplasma gondii*. *Sensors (Basel)* **2023**; 23: 5218. doi:10.3390/s23115218
83. Wang J, Qiu S, Lu H, Yang F, Li G. Microfluidic-based synthesis of crystalline porous materials represented by metal-organic frameworks and covalent-organic frameworks. *Chem Eng J* **2026**; 534: 175029. doi:10.1016/j.cej.2026.175029
84. Jin R, Zhang P, Jiang S, Tian L, Wang Z, Zhu C, et al. Integrated microfluidic sensor array based on mixed-valence cerium metal organic framework for machine learning-assisted identification of antioxidant biomarkers. *J Colloid Interface Sci* **2026**; 719: 140540. doi:10.1016/j.jcis.2026.140540
85. Rashid M, Parsaei S, Ghoorchian A, Dashtian K, Mowla D. A spiral shape microfluidic photoreactor with MOF(NiFe)-derived NiSe-Fe3O4/C heterostructure for photodegradation of tetracycline: mechanism conception and DFT calculation. *J Ind Eng Chem* **2023**; 121: 275-86. doi:10.1016/j.jiec.2023.01.031
86. Li Y, Yu B, Hu Z, Wang H. Construction of direct Z-scheme SnS2@ZnIn2S4@kaolinite heterostructure photocatalyst for efficient photocatalytic degradation of tetracycline hydrochloride. *Chem Eng J* **2022**; 429: 132105. doi:10.1016/j.cej.2021.132105
87. Holzinger A, Langs G, Denk H, Zatloukal K, Müller H. Causability and explainability of artificial intelligence in medicine. *Wiley Interdiscip Rev Data Min Knowl Discov* **2019**; 9: e1312. doi:10.1002/widm.1312
88. Russell SJ, Norvig P. *Artificial Intelligence: A Modern Approach*. Pearson; **2016**.
89. Tsai HF, Podder S, Chen PY. Microsystem advances through integration with artificial intelligence. *Micromachines (Basel)* **2023**; 14: 826. doi:10.3390/mi14040826
90. Mencattini A, Rizzuto V, Antonelli G, Di Giuseppe D, D'Orazio M, Filippi J, et al. Machine learning microfluidic based platform: integration of Lab-on-Chip devices and data analysis algorithms for red blood cell plasticity evaluation in pyruvate kinase disease monitoring. *Sens Actuators A Phys* **2023**; 351: 114187. doi:10.1016/j.sna.2023.114187
91. Sun H, Xie W, Mo J, Huang Y, Dong H. Deep learning with microfluidics for on-chip droplet generation, control, and analysis. *Front Bioeng Biotechnol* **2023**; 11: 1208648. doi:10.3389/fbioe.2023.1208648
92. Zhou Z, Xu T, Zhang X. Empowerment of AI algorithms in biochemical sensors. *Trends Analyt Chem* **2024**; 173: 117613. doi:10.1016/j.trac.2024.117613
93. Molho D, Ding J, Tang W, Li Z, Wen H, Wang Y, et al. Deep learning in single-cell analysis. *ACM Trans Intell Syst Technol* **2024**; 15: 1-62. doi:10.1145/3641284
94. Nan L, Zhang H, Weitz DA, Shum HC. Development and future of droplet microfluidics. *Lab Chip* **2024**; 24: 1135-53. doi:10.1039/d3lc00729d
95. Desir P, Chen TY, Bracconi M, Saha B, Maestri M, Vlachos DG. Experiments and computations of microfluidic liquid-liquid flow patterns. *React Chem Eng* **2020**; 5: 39-50. doi:10.1039/c9re00332k
96. Rizkin BA, Shkolnik AS, Ferraro NJ, Hartman RL. Combining automated microfluidic experimentation with machine learning for efficient polymerization design. *Nat Mach Intell* **2020**; 2: 200-9. doi:10.1038/s42256-020-0166-5
97. Merrin J. Frontiers in microfluidics, a teaching resource review. *Bioengineering (Basel)* **2019**; 6: 109. doi:10.3390/bioengineering6040109
98. Lalegani F, Saffarian MR, Moradi A, Tavousi E. Effects of different roughness elements on friction and pressure drop of laminar flow in microchannels. *Int J Numer Methods Heat Fluid Flow* **2018**; 28: 1664-83. doi:10.1108/HFF-04-2017-0140
99. McIntyre D, Lashkaripour A, Fordyce P, Densmore D. Machine learning for microfluidic design and control. *Lab Chip* **2022**; 22: 2925-37. doi:10.1039/d2lc00254j
100. Fang WZ, Xiong T, Pak OS, Zhu L. Data-driven intelligent manipulation of particles in microfluidics. *Adv Sci (Weinh)* **2023**; 10: e2205382. doi:10.1002/advs.202205382
101. Rose K, Eldridge S, Chapin L. *The Internet of Things: An Overview*. Internet Society; **2015**. p. 1-53.
102. Kopetz H, Steiner W. Internet of things. In: Kopetz H, Steiner W, eds. In: *Real-Time Systems: Design Principles for Distributed Embedded Applications*. Cham: Springer International Publishing; **2022**. p. 325-41. doi:10.1007/978-3-031-11992-7_13
103. Zhang S, Wei S, Liu Z, Li T, Li C, Huang XL, et al. The rise of AI optoelectronic sensors: from nanomaterial synthesis, device design to practical application. *Mater Today Phys* **2022**; 27: 100812. doi:10.1016/j.mtphys.2022.100812
104. Asghari J, Naderi M. Artificial intelligence in nanomaterials studies: a statistical overview. *Nanoscale Adv Mater* **2024**; 1: 73-86. doi:10.22034/nsam.2024.04.01